Deltares

Nuclear Power Plant Site Evaluation: additional locations

Hydrodynamic and meteorological hazards

KNMI
Ministerie van Infrastructuur en Waterstaat

Nuclear Power Plant Site Evaluation: additional locations
Hydrodynamic and meteorological hazards

Client	Ministerie van Economische Zaken en Klimaat
Contact	
Reference	Quotation NPP additional locations, 11209639-001-GEO-0005, d.d. 27 September 2024 Projectplan: NPP additional locations, version 0.2, d.d. 18 March 2025
Keywords	Nuclear Power Plant, hazards, water levels, wind, post-tropical cyclones, precipitation, waves, tsunamis, seiches, temperature

Document control	
Version	1.0
Date	14-04-2026
Project nr.	11209639-016
Document ID	11209639-016-GEO-0002
Pages	47
Classification	Confidential until further notice
Status	Final

Author(s)		

Summary

This document presents an overview of the hydrodynamic and meteorological hazards that can occur in the vicinity of several proposed sites across four locations. The locations are Sloegebied (Borssele), Terneuzen, Maasvlakte II and Eemshaven. The relevant meteorological hazards that have been considered are wind, extra-tropical storms, precipitation, snow and hail. The hydrodynamic hazards that have been identified are tsunamis, seiches, water levels and wave heights.

Data corresponding to these hazards have been gathered, ranging from extreme to more averaged values. Compared to the previous version of the report in which only extreme values for high water levels were reported, additional water level data such as low water extremes as well as highest and lowest astronomical tide levels, and mean high and low waters during neap and spring tides. The effect of climate change and seasonal variability of the data have been considered, if relevant. The data are based on previous studies, literature, existing data and expert judgement, and will be used in preliminary environmental impact studies and will support the site selection of a power plant at the four possible locations.

The data presented here is sufficient for the aim of site selection. If a more extensive quantification of the hazards is required, e.g. in the design stage of the selected site, more , specific studies are required. The effect of the local bathymetry on the spatial variation of wave heights, insight in the local variability of extreme precipitation, insight in the impact of local tsunami waves, quantification of the risk of extra-tropical cyclones are a few examples.

Contents

1 Introduction

1.1 Background

The Dutch government is considering developing two new large nuclear power plants in the Netherlands and is investigating several potential locations. The Ministry of Economic Affairs and Climate Policy of the Netherlands requested Deltares to provide seismological, geological, hydrogeological, meteorological and hydrodynamic data to be used in preliminary environmental impact studies and to support site selection of a power plant at four possible locations: Sloegebied, Terneuzen, Maasvlakte II, and Eemshaven. The four locations are indicated in Figure 1.1.

Figure 1.1 Possible locations for a nuclear power plant at Terneuzen (left upper), Eemshaven (right upper), Sloegebied (left lower) and Maasvlakte II (right lower). Source: 'concept notitie reikwijdte en detailniveau (Plan-MER locatiestudie twee nieuwe kerncentrales)'.

Within the scope of this study are the external hazards as described in Chapter 5 of IAEA-SSR-1[1]:

- Evaluation of extreme meteorological hazards.
- Evaluation of rare meteorological events.
- Evaluation of flooding hazards.
- Changes of hazards and site characteristics with time.

This studies will focus on the hazard assessment and the data required to perform a reliable assessment of hazards. As the design of the facility and the exact location of the facility are yet unknown, this study does not include an assessment of the vulnerability, the risk of damage, or failure of the facility in relation to the identified hazards.

[1] International Atomic Energy Agency – Specific Safety Requirements

1.2 Objective

The objective of this study is to make an inventory of all relevant meteorological and hydrodynamic hazards that can occur at the potential locations at Sloegebied, Terneuzen, Maasvlakte II, and Eemshaven, based on a literature study as well as expert judgements.

In addition to the assessment of the hydrological and meteorological hazards at this site, an initial screening of the extreme statistics of wind speed, waves, and water levels in the direct vicinity of the plant was assessed, as this was considered relevant as input for preliminary environmental impact studies and site selection. The data will be used by parties that will carry out these studies.

The selection of hydrological and meteorological hazards, that were addressed, was based on the Specific Safety Guide regarding these hazards, set up by the International Atomic Energy Agency (IAEA, 2011). The present report addresses the following meteorological and hydrodynamic hazards and resulting variables, with reference to the IAEA articles and the experts having contributed to these subjects:

- Wind speed (article 2.7 in IAEA, 2011) – Jacco Groeneweg (Deltares), Peter Siegmund (KNMI).
- Post-tropical cyclones (article 2.8) – Peter Siegmund.
- Extreme precipitation (article 2.7) – Peter Siegmund.
- Tsunamis (article 2.11) – Reimer de Graaff (Deltares).
- Seiches (article 2.11) – Martijn de Jong (Deltares).
- Extreme high and low water levels and wave heights (article 2.11) – Jacco Groeneweg.
- Highest and lowest astronomical tide levels, as well as mean high and low waters during neap and spring tides – Reimer de Graaff (Deltares)..
- Temperature (article 2.6) – Peter Siegmund.

The report is a co-production of KNMI and Deltares.

2 Hazard assessment

2.1 Extreme wind conditions

In the Netherlands wind speed has been measured for decades at various KNMI stations near the coast and inland. These measurements have been used to derive extreme wind speeds. The extreme statistics have been defined based on the annual maxima of the so-called potential wind speed[2]. For the safety assessment and design of dunes and dikes along the Dutch coast the tools gathered within WBI2017, the so-called legal assessment tools are applied. The probability distributions for both potential wind speed and water level are part of WBI2017, and are useful for the present study. The reference date of the statistical distributions is 2023. De Valk and Van den Brink (2023) updated the wind and water level statistics along the Dutch coast, based on approximately 8000 years of simulated data of wind and water levels in the North Sea, that was available from seasonal forecasts. Since the updated statistical values have not yet been established, the original values will be considered here.

A selection of the locations for which wind speed statistics is available has been presented in Appendix A. Although some locations are closer to the plant locations we prefer wind measurement locations that are not hindered by land effects. As a consequence the wind statistics may be conservative for the plant locations. The wind statistics at Cadzand are considered relevant for the plant locations Sloegebied and Terneuzen. The wind statistics at Hoek van Holand are considered to be representative for Maasvlakte II and West-Terschelling for Eemshaven.

Based on the directional extreme value distribution for the wind speed, a omni-directional wind speed exceedance chart has been constructed (see Appendix A for further details). The values for return periods ranging from 10 to 1.000.000 years are presented in Table 2.1.

Table 2.1 The wind speed being exceeded for various return periods [m/s].

Return period [years]	**Cadzand (Sloehaven and Paulinapolder)**	**Hoek van Holland (Maasvlakte II)**	**West-Terschelling (Eemshaven)**
10	25.5	24.5	25.8
100	30.0	28.6	29.9
1000	34.6	32.7	34.0
10.000	39.3	36.8	38.1
100.000	44.1	41.1	42.3
1.000.000	49.1	45.3	46.8

2.1.1 Effect of climate change

In 2023 KNMI presented new climate scenarios. In summary, changes in wind speed and wind directions will be limited. The expected amount of days with an average wind speed of at least 14 m/s (Bft 7) slightly decreases. Also the wind directions slightly change, resulting in less days with strong north-western wind.

[2] The potential wind speed is a reference wind speed , free of local effects. It is obtained by correcting for the effect of different roughness, than the one of cut grass, and measuring height, other than 10 m.

2.1.2 Seasonal variability

From https://daggegevens.knmi.nl/ wind related data has been downloaded for the period 2015-2024, spread over the four seasons. From this data the averaged and highest daily-averaged wind speed over the seasons were computed, as well as the highest hourly-averaged wind speed per day and highest wind gust per day over the same seasons. For the KNMI stations Vlissingen, Hoek van Holland and Lauwersoog these values are presented in Table 2.2. The locations differ from those for which the extreme value statistics were presented (Table 2.1). This is not considered a problem, since the seasonal data give a general picture of the seasonal variability.

Table 2.2 Averaged and highest daily-averaged wind speed, highest hourly-averaged wind speed and highest wind gust per day at Vlissingen, Hoek van Holland and Lauwersoog for four seasons.

		Vlissingen	Hoek van Holland	Lauwersoog
averaged daily-averaged wind speed	Winter	7,3 m/s	8,0 m/s	6,8 m/s
	Spring	5,9 m/s	6,8 m/s	6,5 m/s
	Summer	5,5 m/s	6,2 m/s	5,7 m/s
	Autumn	6,1 m/s	7,0 m/s	5,8 m/s
highest daily-averaged wind speed	Winter	17,5 m/s	17,8 m/s	18,2 m/s
	Spring	16,7 m/s	17,3 m/s	17,7 m/s
	Summer	14,7 m/s	15,0 m/s	13,2 m/s
	Autumn	18,0 m/s	16,1 m/s	16,8 m/s
highest hourly-averaged wind speed per day	Winter	28 m/s	30 m/s	23 m/s
	Spring	23 m/s	21 m/s	23 m/s
	Summer	22 m/s	22 m/s	22 m/s
	Autumn	23 m/s	23 m/s	22 m/s
highest wind gust per day	Winter	39 m/s	40 m/s	34 m/s
	Spring	34 m/s	37 m/s	31 m/s
	Summer	29 m/s	30 m/s	30 m/s
	Autumn	32 m/s	33 m/s	33 m/s

For all stations the highest daily-averaged or maximum values are obtained during winter, in summer the lowest. This is the main reason to apply data from autumn and winter to derive the wind statistics to be applied in WBI2017. The highest hourly-averaged wind speed and wind gusts per day tend to occur in Hoek van Holland and Vlissingen. Lauwersoog is more sheltered by the Wadden islands from the North Sea.

2.2 Post-tropical cyclones

Appendix B provides the literature review carried out by the KNMI. Here the main findings are presented.

Tropical cyclones, or hurricanes, are extremely powerful storms that can develop over areas with warm sea water. Some tropical cyclones develop off the African West Coast and move northward along the US East Coast, losing their tropical character and turning into an extra-tropical storm. At the height of Newfoundland these post-tropical cyclones are carried by the jet stream towards Europe, and on the way they can regain strength under favourable conditions. A warming climate might contribute to increased frequency and intensity of post-tropical cyclones in Europe.

A study on European cyclones with tropical origin in reanalysis data revealed that in the period 1979-2013 53 hurricanes have entered the European area. A very few of them still had hurricane strength when they hit the western part of the British Isles. The Netherlands has never been hit by a post-tropical cyclone with hurricane force (Beaufort 12, wind speeds over 36 m/s). From the observational data the conclusion is therefore that the risk of the Netherlands being hit by a post-tropical cyclone with Beaufort 12 is negligible.

In 2017 Europe was hit by hurricane Ophelia, which due to high water temperatures regained strength prior to passing the Irish coastline. Ophelia can be considered as a showcase for cyclone characteristics in a warmer climate. The British Isles are not necessarily the only area exposed to off-track tropical cyclones: according to a model simulation, Ophelia could just as well have squeezed through the Straits of Calais to reach the Dutch coast with hurricane force winds. In October 2024 post-tropical cyclone Kirk caused significant damage in portions of Western Europe. In early predictions the cyclone track passed the Netherlands, but in later predictions and in reality the cyclone made landfall in south-west France.

Further climate studies confirmed the increased risk of Western Europe to be hit by a extra-tropical storm that originates from hurricanes. Further research is however required to quantify this risk in more detail. Therefore, the hazard is not considered further within this study.

2.3 Extreme precipitation with the potential to induce local flooding

Appendix B provides the literature review carried out by the KNMI. Here the main findings are presented.

A literature study is carried out regarding the precipitation risk, as extreme precipitation (both intensity and duration) may lead to local flooding. These results are representative for the entire country of the Netherlands.

Frequency statistics of (extreme) rain in the Netherlands is provided by STOWA (2019) as the amount of rain for a given rainfall duration (two hours to eight days), which is exceeded with a certain frequency (Figure 2.1). The average amount of precipitation per year in the Netherlands increased by 9% between 1961-1990 and 1991-2020. However, the amount of rainfall during extreme wet days increased by 15%. In a warmer climate, the atmosphere can contain more water vapor and, therefore, extreme showers are expected to occur more often in the future.

In the KNMI’23 climate scenario’s precipitation extremes increase throughout the year in all scenario’s, except in the Ld-scenario (low emissions, dry variant) in winter. Relative to the refence period 1991-2020, the winterly 10-day amount that is exceeded once in 10 years changes by -2 to +2% around 2050 and by -2 to +15% around 2100. Positive changes indicate an increase and negative changes a decrease. In summer the daily amount exceeded once in 10 years increases by +4 to +11% around 2050 and +4 to +31% around 2100. The maximum hourly amount per year in summer increases by +4 to +11% around 2050 and +4 to +31% by 2100.

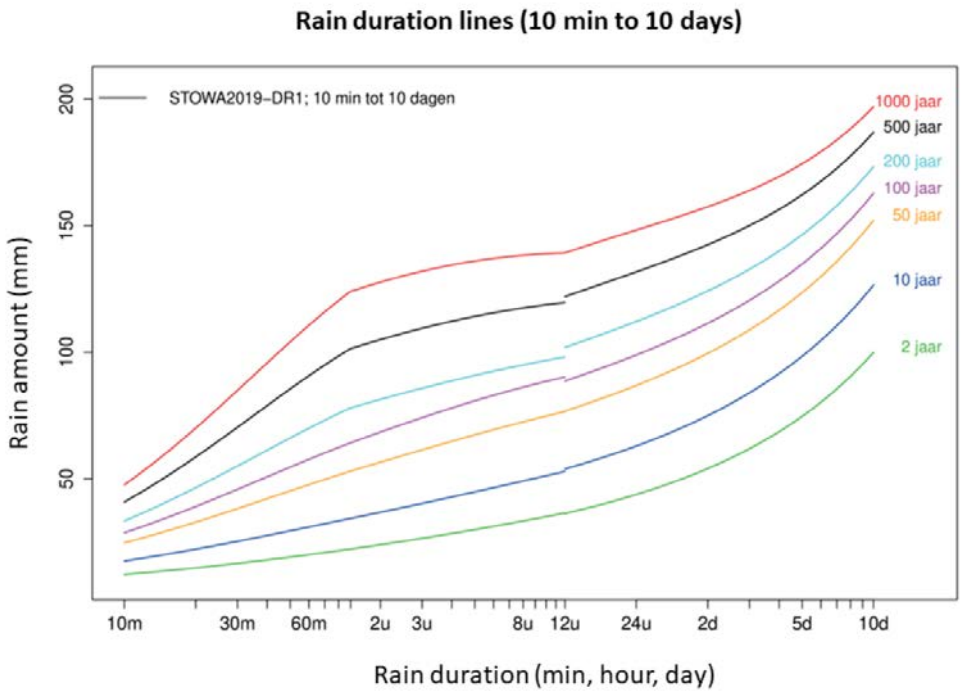

Figure 2.1 Rain duration lines based on precipitation observations in the Netherlands for the whole year. Source: STOWA (2019).

2.3.1 Hail

Due to the lack of long, high-quality measurements, little is known about possible trends in the frequency and intensity of hail. Because there is more water vapor in the atmosphere and vertical motions intensify, the largest hail stones are likely to become even larger. Regional climate models have been used to determine the frequency of hail with a diameter of 50 mm or more for Europe (Rädler et al., 2019). In the Netherlands, the frequency is highest in the southeast, about once every 15 years. At the end of this century, this frequency will increase, in case of an average global warming of 2 degrees, to about once every 10 to 12 years.

2.3.2 Snow

The number of days with snowfall in the Netherlands increases from the south-west to the north-east, from about 14 days per year in Zeeland (average for 2003-2020) to 24 days in the north-east. The KNMI'23 scenario's do not provide information for snowfall in the future, but given the future warming of the Netherlands the frequency of snowfall is expected to decrease. As a relative proxy for the frequency of snowfall one might use the frequency of frost days, on which the minimum temperature is below 0°C. Around 2050 the frequency of frost days in De Bilt is expected to be decreased by 26% to 44% relative to the reference period 1991-2020 (KNMI, 2023).

2.4 Tsunamis

2.4.1 General description

Tsunamis are waves propagating in the sea because of a sudden vertical displacement of the water column. Offshore, tsunamis can have wavelengths of up to a few 100 km's and wave amplitudes of usually less than 1 m. When tsunami waves approach the coast, the propagation speed decreases and the amplitude increases, potentially leading to coastal inundation.

Potential sources of tsunamis reaching the Dutch coast may be from subsea earthquakes at (distant) subduction zones or at (local) fault zones, subsea landslides, erupting or collapsing volcanoes, meteorites, or fast-propagating storm fronts along the coast (meteo-induced long waves meteotsunamis).

The literature study (see Appendix C) on tsunamis potentially affecting the Dutch coast showed that the probability of a destructive tsunami reaching the Dutch coast is considered to be very low, because the North Sea is not in a tsunami-prone region and because tsunamis that do propagate from remote areas will largely dissipate due to the shallow waters of the southern part of the North Sea. Tsunamis affecting the Dutch coastline are either formed because of a landslide in the northern part of the North Sea or a local earthquake-generated tsunami in the southern part of the North Sea. Both are expected to result in maximum estimated tsunami wave heights of between 1.5 m to 2 m. However, the probability of occurrence of these events is very low (about once in 100.000 years). Other tsunamigenic sources, such as from earthquakes at remote subduction zones, volcanoes or meteorites, are not expected to result in significant tsunami wave heights at the Dutch coast. Most probable cause of tsunami wave heights of up to 1 m are from fast moving storm fronts (meteotsunamis, see also Section 2.5).

2.4.2 Maximum expected tsunami wave heights at the considered sites

The maximum expected tsunami wave heights at each of the four sites (based on expert judgement and with reference to the literature study in Appendix C) are presented below.

Terneuzen
It is expected that tsunami wave heights will be lower at the Terneuzen site compared to the values reported for the Dutch coast in Section 2.4.1. The expected further reduction of estimated tsunami wave height at the Terneuzen site is motivated by dissipation of a tsunami wave in the relatively shallow Western Scheldt estuary. However, no quantified data or information is yet available to confirm this.

Sloegebied
It is expected that tsunami wave heights will be lower at the Sloegebied site, for the same reason as Terneuzen.

Maasvlakte II
It is expected that tsunami wave heights will be similar to the values reported for the Dutch coast in Section 2.4.1, because of its location at the Dutch coast.

Eemshaven
It is expected that tsunami wave heights will be lower at the Eemshaven compared to the values reported for the Dutch coast in Section 2.4.1. The expected further reduction of estimated tsunami wave height at Eemshaven site is motivated by dissipation of a tsunami wave in the shallow Wadden Sea and Ems estuary. However, no quantified data or information is yet available to confirm this.

2.5 Seiches

2.5.1 General description

Seiches are standing, resonant long waves inside (semi-)enclosed basins. If they occur, then they are linked to specific oscillation periods that are coupled to the local geometry. Seiches can cause safety and operational issues, for example inside ports and harbours, and they can add to the hydraulic loading on coastal structures and other infrastructural developments.

Seiches can occur in the estuaries and ports along the Dutch coast (see Deltares, 2015a, 2016, 2017 for a nation-wide inventory and quantification of potential Dutch seiching locations). Seiches in (semi-)enclosed basins along the Dutch coast are triggered by long waves that are generated on the North Sea and that propagate towards the Dutch coast. Those events are generated by passing low-pressure systems and cold fronts. All measured seiche events coincide with a storm, but not all storms lead to seiche events. This is linked to a critical level of instability in the atmosphere (see De Jong, 2004, and references therein).

At coastal locations without a local geometry feature (port or other bay shape), a local seiche is not triggered and the incoming long waves from the North Sea pass an area un-amplified. Due to dissipation, the amplitude will become lower as the long waves propagate further into a coastal bay area or estuary, possibly partially compensated by a narrowing geometry, where applicable (e.g. a funnel-shaped estuary).

In (international) literature, the meteorologically generated long waves we consider here are generally referred to as 'meteotsunamis'. Following that labelling, these events are often classified as part of tsunamis (Section 2.4.1). Here we consider them as a separate phenomenon. This is because this type of long-wave events has a distinctly different and much more local cause than 'regular' tsunamis ((distant) earthquakes, landslides) and occur much more frequently, especially when considering the situation in The Netherlands, albeit generally with limited amplitudes.

2.5.2 Seiche characteristics at the considered sites

Deltares (2015a, 2016, 2017) gives extensive information on typical amplitudes of oscillations on large water bodies within The Netherlands. That series of studies considers water level measurements at a large set of observation locations throughout The Netherlands and derives first estimates of statistics of extreme local seiche amplitudes. In some cases the available measurement locations are present within a lake, port or bay geometry, directly representing local seiche events. In other cases the available measurement locations are in open water and describe for a region the incoming long wave characteristics only. Such measurements will be directly representative for an open location along the shoreline but if a local port geometry is to be assessed, then an estimate of the local amplification needs to be added. Here that effect is estimated based on expert judgement. If needed, a more detailed derivation of local amplifications could be made using numerical modelling per considered location.

The descriptions included later in this section motivate the estimates of the local long-wave and seiche-characteristics at the different considered sites, using information from the earlier nation-wide study series (2015-2017), where possible combined with other literature sources and expert judgement interpretations. Table 2.3 summarizes the results.

Table 2.3 Summary of estimated long-wave and seiche characteristics at the potential plant sites.

Location	Representative (extreme) seiche or long-wave amplitude (m)	Oscillation periods
Terneuzen	0.3	1 – 1.5 h
Sloegebied	0.3 – 0.6	1 – 1.5 h, and an unknown local seiche period
Maasvlakte II	0.3 – 0.8	30 minutes – 1.5 h
Eemshaven	0.3 – 0.5	15 – 30 minutes

Note that, where available, the values listed represent estimates of local amplitude magnitudes for long waves and seiches for a 4000 – 10000 year return period, based on a preliminary statistical derivation in the report series (2015-2017) mentioned earlier. The return period associated with these values could be derived more accurately in more thorough statistical analyses. Furthermore, the values listed have been estimated without considering correlations with other relevant parameters. For example, although there may be a (small) positive correlation with wind-induced surge, the return period of these amplitudes occurring at the same time as an extreme surge level may be much longer. Or conversely, considering the (limited) correlation between wind-induced surges and seiche-amplitudes in a statistical analysis will generally lead to lower local seiche amplitudes for a given return period, as was illustrated in Deltares (2015b,c) for the basins along the Western Scheldt at Terneuzen. Moreover, port quays may flood during extreme surge and seiche events, which will result in significant energy losses in the seiche response that will limit the magnitude of an oscillation within a port geometry. This effect was considered in some of the earlier studies on seiching along the Dutch coast, most extensively for IJmuiden (Deltares, 2014a) and for Rotterdam (Deltares, 2014b). The estimated amplitude ranges provided include such influences as part of the expert judgement interpretations where possible, but a more detailed assessment would be needed to fully represent such effects (including numerical modelling).

Terneuzen
The Terneuzen site is foreseen directly along the Western Scheldt. This means that long waves are considered for this location without a local effect of resonance that may otherwise occur in (semi-)enclosed basins. Based on a literature review described as part of Deltares (2015b,c), the best estimate currently available of a representative long wave amplitude at Terneuzen is around 0.3 m, comparable to the estimate provided for the Western Scheldt outside of the port of Vlissingen (Tiessen et al., 2024).

Sloegebied
For the potential location in the Sloegebied, the relevant long wave (or seiche) amplitude will depend on whether the site will border the inner port basin or the outer shoreline along the Western Scheldt. Outside of the port the amplitude may be limited to around 0.3 m (Tiessen et al., 2024), but amplification may occur inside the port. Analyses of the port basins present along the Western Scheldt at Terneuzen (Deltares, 2015b,c) have shown that most long-wave energy is present in this area at much longer time scales (around 1 – 2h) than the resonant periods related to the geometry of local port basins (for example around 10 minutes, inside the basins in front of the lock compound of Terneuzen). This means that some effect is possible, but that a very strong amplification is generally not expected, given that the oscillation time scales of the forcing and of the response do not match. For now, the combination of different local influences has been estimated to correspond roughly to a doubling in amplitude, resulting in a range of relevant local amplitudes of seiches of 0.3 – 0.6 m.

Rotterdam - Maasvlakte II (MV2)
The possible site at MV2 is foreseen directly within the perimeter of MV2 and on the other side the plant would border the inner port basin (Princes Ariana Basin). The outer perimeter of MV2 will experience the unamplified incoming long-wave amplitude, while inside the basin a (higher) seiche-response may occur. In this case the oscillation periods of the incoming long waves may match the periods of seiches inside the Rotterdam port basins, potentially leading to an amplification of the incoming amplitudes from open sea. These considerations result in an estimated range for the local seiche amplitudes of 0.3 – 0.8 m.

Note that the design of the MV2 reclamation area included an allowance for seiching as part of determining the design construction height of that man-made land area (details available at original contractor consortium partners and Port of Rotterdam). Deltares has contributed with

an exploratory study of seiche characteristics during extreme conditions (De Jong et al., 2006), which has aided the Port in selecting a design value for seiche amplitudes. This would mean that constructing the new power plant at the (design) elevation of MV2 would already include an allowance for the local occurrence of seiching. In this way the higher local amplitude value estimated for seiches at this site may not directly be a drawback for selecting this location.

Eemshaven
The two potential sites at Eemshaven both directly border the Wadden Sea. The eastern option at this location also borders the inner port basin (Wilhelmina Basin). Along the outer perimeter, only unamplified long waves will occur, while the port basin may enhance local seiche amplitudes. Rijkswaterstaat (1980) reports for inside the Wilhelmina Basin a local amplitude of 0.35 m at a period of around 30 minutes, while analyses described in Deltares (2017) show that representative amplitudes inside the port may be around 0.5 m. For now, this leads to an estimated range of 0.3 – 0.5 m at these potential plant sites, depending on whether the site will also border the port basin or only the outer shoreline.

2.6 Water levels and wave heights

As mentioned in Section 2.1, for the safety assessment and design of dunes and dikes along the Dutch coast, use is made of the tools gathered within WBI2017, the so-called legal assessment tools. The probabilistic tools within WBI2017 are Riskeer and Hydra-NL. The latter provides hydraulic loads, whereas the first includes descriptions of failure mechanisms and can be used to determine to determined flood probabilities. For the present study we use Hydra-NL.

The hydraulic loads in terms of local water levels and wave conditions can be determined for arbitrary probabilities of exceedance. Details about the derivation of the extreme water levels and wave heights can be found in Appendix A.

2.6.1 Extreme water level

Hydra-NL has been used to determine the local marginal water level statistics at output locations in front of the four plant locations. In Table 2.4 the water levels for the return periods from 10 to 1.000.000 years are presented at the four plant locations. Since extreme water levels for return periods of 1 year are not included in Hydra-NL, they have been estimated based on linear extrapolation of the 1 in 10 and 100 year values and added to the table.

Table 2.4 The water level being exceeded for various return periods [m + NAP].

Return period [years]	Terneuzen	Maas-vlakte-II	Sloehaven West	Sloehaven East	Eemshaven West	Eemshaven East
1*	3.5	2.4	3.3	3.4	2.9	3.0
10	4.1	3.1	3.9	4.0	3.7	3.7
100	4.7	3.7	4.5	4.6	4.4	4.5
1000	5.3	4.4	5.1	5.2	5.1	5.2
10.000	6.0	5.2	5.7	5.8	5.7	5.9
100.000	6.7	6.0	6.3	6.5	6.4	6.5
1.000.000	7.4	6.9	7.0	7.2	7.1	7.2

* *based on extrapolation*

The spatial variation at most plant locations is small, as presented in Appendix A.3, and is in the order of centimeters. Since the water levels are presented in one decimal, the spatial

variation at the site location is neglected for Terneuzen and Maasvlakte-II. At the harbours of Sloehaven and Eemshaven the difference between the eastern and western sides is in the order of 1-2 dm. Therefore water levels at both sides are presented for those locations.

As mentioned in Section 2.1 the water level statistics were updated by De Valk and Van den Brink (2023). Since the updated statistical values have not been established yet, the original values are considered in this study.

2.6.2 Sea level rise

In 2023 KNMI published the projected effects of climate change for four different scenarios (see KNMI, 2023). The projected sea level rise for 2050 was estimated between +16 cm and +38 cm (depending on the scenario considered), whereas sea level rise was expected to accelerate in the later stages of the century resulting in a sea level rise between +26 cm to +124 cm for 2100. The bandwidth has increased significantly for 2100, for a large part due to the uncertainty in the rate of mass-loss of the Antarctic ice sheet.

2.6.3 Additional water level data

Time series of the measured water levels (relative to NAP) until the end of March 2025 have been made available by Servicedesk Data of Rijkswaterstaat. Table 2.5 shows the starting date of the time series, most of them starting in 1950. Measurements at Amaliahaven only started after realization of Maasvlakte II. Note that in the early years 3 hour averaged values were stored, the last decennia 10 minute averages and the last couple of years for Vlissingen and Hoek van Holland even 1-minute values. The time series have not been homogenized for this study.

For illustration, Figure 2.2 shows the water levels measured at Hoek van Holland. The figure includes the maximum over the entire time series as well as over the last 10 years. These maxima have also been included in Figure 2.2 for all locations.

Table 2.5 Duration and maxima (over entire range and over last 10 years) of measured water level (in m+NAP) at five locations.

Location	Starting date	Maximum over entire time series		Maximum over last 10 years	
		Water level	Date	Water level	Date
Eemshaven	29-12-1978	4.19	01-11-2006 06:00	3.51	22-12-2023 06:30
Amaliahaven	24-04-2013	3.25	06-12-2013 05:00	3.22	21-12-2023 22:10
Hoek van Holland	01-01-1950	3.81	01-02-1953 04:40	3.14	21-12-2023 22:19
Terneuzen	01-01-1950	4.52	01-02-1953 02:40	3.96	03-01-2018 14:40
Vlissingen	01-01-1950	4.53	01-02-1953 03:40	3.61	03-01-2018 14:31

The 1953 storm led to the highest water levels in the southern part of the Netherlands. The time series at Eemshaven start in 1978 and show the largest water level during the Allerheiligen storm of 2006. The maxima over the last 10 years are 0.6 – 0.9 m lower than over the entire series, most maxima occurring during Storm Pia in December 2023.

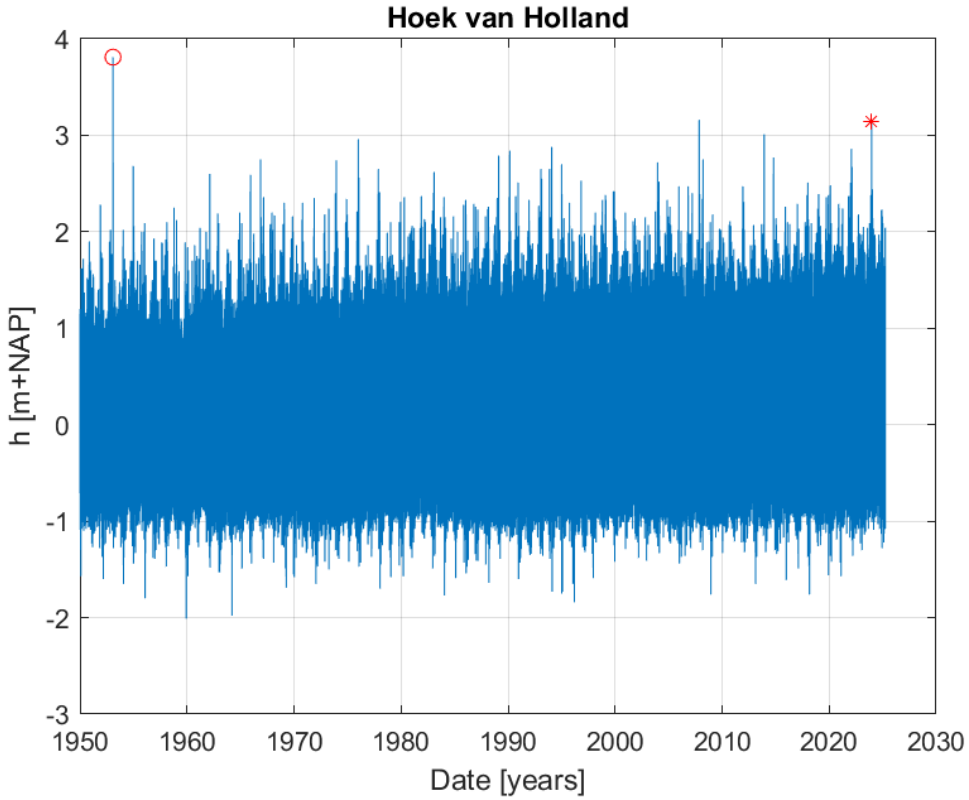

Figure 2.2 Measured water level (in m + NAP) at Hoek van Holland, 'o' indicating the maximum water level over the entire period, '' over the last 10 years.*

Extreme low waters (not included in Hydra-NL) were assessed for all locations, except Amaliahaven, by fitting a Gumbel distribution through a cluster of peaks (in this case the lowest observed water levels) using Deltares statistical data processing toolbox ORCA. For Amaliahaven the extreme low waters were assessed differently, because the duration of the measured time series (12 years) is too short for extreme value analysis. For this location the extreme low water levels were assessed by correlating the observed peak low waters at Amaliahaven with simultaneously occurring peak low water levels at Hoek van Holland. The resulting regression equation (y = 1.05x – 0.08) was used to assess the extreme low water levels in Amaliahaven for all return periods. Although not presented in the table, note that the extreme water levels for return periods of more than 100 years will have an increasingly large uncertainty. Note that the extrapolation of the extreme low waters are irrespective of the local water depths.

Table 2.6 The low water level being exceeded for various return periods [m + NAP].

Return period [years]	Terneuzen	Vlissingen	Amaliahaven	Hoek van Holland	Eemshaven
1	-2.7	-2.6	-1.3	-1.2	-2.2
10	-3.1	-3.0	-1.9	-1.7	-2.8
100	-3.4	-3.3	-2.2	-2.0	-3.3
1000	-3.8	-3.6	-2.6	-2.4	-3.7
10.000	-4.1	-3.9	-2.9	-2.7	-4.2
100.000	-4.4	-4.2	-3.3	-3.1	-4.6
1.000.000	-4.8	-4.5	-3.7	-3.4	-5.1

Highest and lowest astronomical tide levels, as well as the mean high and low waters during neap and spring tides (MHWS, MHWN, MLWN, MLWS), were assessed also from the Rijkswaterstaat water level measurements. The procedure was as follows for each of the five measurement locations:

1. perform harmonic analysis on the measured water level time-series to assess the amplitudes and phases of a large number of tidal constituents (e.g. including M2, S2, K1 and O1);
2. make a prediction for 19 years (to include a full tidal cycle of 18.6 year) with the tidal constituents from step 1;
3. assess the maximum (HAT) and minimum (LAT) water levels within the 19 year prediction.

The resulting tide levels for the five locations are given in Table 2.7.

Table 2.7 The HAT and LAT levels [m + NAP].

Return period [years]	Terneuzen	Vlissingen	Amaliahaven	Hoek van Holland	Eemshaven
HAT	3.4	3.1	1.9	1.8	2.0
MHWS	2.9	2.6	0.7	0.7	1.5
MHWN	1.7	1.5	0.4	0.4	1.0
MSL	0.2	0.1	0.1	0.1	0.1
MLWN	-1.4	-1.4	-0.4	-0.4	-1.0
MLWS	-2.1	-2.0	-0.7	-0.6	-1.6
LAT	-2.7	-2.6	-1.0	-1.0	-2.1

2.6.4 Extreme wave height

As presented in Appendix A.2 the extreme value distribution for wave height is strongly dependent on the bed level on the seaward side of the study-location and on the dike orientation. Wave breaking at the foreshore increases with more shallow water depths and reduces the wave height at the coastal defenses surrounding the proposed sites. E.g. the 1/10.000-year wave height exceedance values vary from 2.0 m to 2.6 m at Terneuzen to 7.6 m to 10 m at Maasvlakte II. Further details regarding the layout near the potential sites (primarily its location and surrounding bed levels) can help reduce this uncertainty.

2.7 Temperature, Drought & heatwaves

The maximum and minimum air temperatures are computed from the KNMI daily observation archive available at https://daggegevens.knmi.nl/. This archive is also used to compute the highest and lowest values for the long-term (10 and 30 days) and short-term (1, 2 and 5 days) temperature averages. Also the relative humidity and sea level pressure values are computed from this archive. 100 year-return periods for maximum and minimum temperature are computed by fitting a GEV (Generalized Extreme Value) distribution to the highest annual maximum temperature and lowest annual minimum temperature, using the tool ‘Trends in return times of extremes’ of the KNMI Climate Explorer https://climexp.knmi.nl/.

The parameters are computed for the KNMI weather stations in Vlissingen, Hoek van Holland and Eelde. There is also a weather station in Westdorpe near Terneuzen. Since the measurements start in 1991, while for Vlissingen in 1906, the Vlissingen station is also used for Terneuzen. At station Hoek van Holland measurements are available since 1971, with a gap from 1981 to 1990. These are used for Maasvlakte II. For Eemshaven the measurements

at KNMI station Eelde are used. At this station the measurements have been carried out since 1906. The temperature related parameters at these locations are presented in Table 2.8.

Table 2.8 Summary of temperature related data (1/100 air temperature from climate of 2024, with smoothed global mean temperature as the covariate).

Parameter		Vlissingen	Westdorpe	Hoek van Holland	Eelde
Air Temperatures [°C]	Max	37.3 (25-7-2019)	40.6 (25-7-2019)	38.9 (25-7-2019)	36.9 (24/25-7-2019)
	Min	-18.9 (21-2-1956)	-14.9 (25-1-2013)	-13.0 (2-1-1997)	-22.9 (16-2-1956)
1/100 year-Air Temperature and 95% range [°C]	Max	38.1 [36.3 - 40.0]			38.2 [36.9 - 39.3]
	Min	-14.6 [-19.0 - -11.8]			-14.5 [-18.7 - -11.8]
Highest N-day averaged temperature [°C]	N=1	27.9 (2014)		20.3 (2022)	28.3 (2019)
	N=2	27.0 (2020)		27.7 (2019)	28.2 (2019)
	N=5	26.3 (2020)		25.6 (1975)	26.3 (2019)
	N=10	22.9 (2022)		24.0 (2020)	24.1 (2020)
	N=30	22.2 (2006)		21.5 (2006)	21.5 (2006)
Lowest N-day averaged temperature [°C]	N=1	-11.8 (1938)		-10.5 (1997)	-19.4 (1956)
	N=2	-11.4 (1938)		-10.0 (1997)	-16.1 (1979)
	N=5	-10.3 (1929)		-8.0 (1996)	-13.2 (1942)
	N=10	-8.6 (1929)		-6.8 (1996)	-12.5 (1942)
	N=30	-4.6 (1962)		-2.7 (1996)	-9.0 (1942)
Relative humidity [%]	Max	98 (21-2-1956)	99 (25-1-2013)	82 (2-1-1997)	93 (16-2-1956)
	Min	27 (25-7-2019)	21 (25-7-2019)	28 (25-7-2019)	32 (24-7-2019)
Sea Level Pressure [hPa]	Max	1049.1 (1932)		1048.2 (2020)	1053.0 (1907)
	Min	954.4 (1985)		954.8 (1985)	954.2 (1983)

Over the period 2015 – 2024 the daily averaged values for the temperature, relative air humidity sea level pressure and wind speed have been downloaded from https://daggegevens.knmi.nl/, as well as the maximum and minimum daily temperature, precipitation per day and highest hourly-averaged wind speed and wind gust per day. For all parameters the averaged value, as well as the highest and lowest value over the entire period are presented in Table 2.9.

Table 2.9 Summary of temperature related data over the period 2015-2024 at three KNMI stations. The averaged, lowest and highest values over that period are presented.

	Vlissingen			Hoek van Holland			Eelde		
	averaged	highest	lowest	averaged	highest	lowest	averaged	highest	lowest
Daily-averaged temperature [ºC]	12	27.9	-4.5	11.8	30.3	-5.8	10.5	28.3	-7.8
Maximum daily temperature [ºC]	14.8	37.3	-3	15	28.9	-3.7	14.7	36.9	-5.4

	Vlissingen			Hoek van Holland			Eelde		
Minimum daily temperature [ºC]	9.4	22.2	-6.2	8.6	21.2	-8	5.9	21.5	-12.6
Daily-averaged relative air humidity [%]	79	100	43	79	100	34	82	100	42
Daily-averaged sea level pressure [hPa]	1016	1047	972	1016	1047	972	1015	1046	974
Precipitation per day [m]		78			46			47	
Daily-averaged wind speed [m/s]	6.2	18		7	17.8		4	12.3	
Highest hourly-averaged wind speed per day [m/s]		28			30			21	
Highest wind gust per day [m/s]		39			40			34	

Drought is measured by KNMI by the precipitation deficit, which is approximately the sum of potential evaporation minus precipitation, starting the sum on 1 April, up to 30 September. The precipitation deficit has a maximum in the end of the summer. The average of these maxima over the years 1991 till 2020) is 160 mm, see https://www.knmi.nl/klimaatdashboard.

In De Bilt there have been 30 heatwaves since 1901, of which 14 occurred after 2000, see https://www.knmi.nl/nederland-nu/klimatologie/lijsten/hittegolven.

3 Summary and recommendations

This report provides an overview of the various hydro- and meteohazards that can occur in the vicinity of the proposed nuclear power plant sites of Sloegebied, Terneuzen, Maasvlakte II and Eemshaven. The data presented in this document are based on previous studies, literature, existing data and expert judgement.

3.1 Summary

- Extreme wind conditions: The extreme value distribution of the wind speed is presented in this document, based upon measurements at Cadzand, Hoek van Holland and West-Terschelling, for example the 1/10.000-year extreme wind is 37 – 39 m/s at these locations. The foreseen effect of climate change is small (few percents) compared to these values.
- Extra-tropical cyclones: The Netherlands has never been hit by a post-tropical cyclone with Beaufort 12 according to measurements. However, recent model studies have shown that it is possible for powerful extra tropical cyclones to hit the Netherlands, and that the probability will increase with climate change. Further research is however required to quantify this risk. Therefore, the hazard is not considered further within this study.
- Precipitation: The extreme value distribution of the precipitation presented here is based upon measurements across the Netherlands. Climate studies also provide quantified changes for precipitation for winter and summer conditions, for various time-horizons.
- Tsunamis: The probability of a destructive tsunami reaching the Dutch coast is low (1/100.000 per year) and can result in maximum wave heights between 1.5 m and 2 m.
- Seiches: The best estimate currently available of the long wave amplitude coming from sea that could potentially create seiches is 0.30 m. In absence of a (port) geometry, a resonant (seiche) response may not be triggered, and this amplitude will not be amplified. Inside Sloehaven, Amaliahaven (MV2) and Eemshaven an amplification of a few decimeters is realistic.
- Water level: The extreme value distribution of the water level is presented in this document, based upon measurements at Vlissingen, Hoek van Holland and Lauwersoog over a long period. For example the 1/10.000-year extreme water levels are 5.2 - 5.5 m + NAP. On top of that, the expected sea level rise for 2100 is potentially up to 1.2 m by 2100.
- Wave height: wave conditions show a strong spatial variation along the proposed sites; the 1/10.000-year wave height exceedance value at Terneuzen and Maasvlakte II vary from 2.0 m to 2.6 m and 7.6 m to 10 m respectively.

3.2 Recommendations

Two aspects are critical for a more accurate assessment of the potential meteorological and hydrodynamical hazards facing the four potential site locations.

Firstly, the current study is based on existing data, literature and expert judgement. For a more extensive quantification of the hazards, specific studies are required:

- Numerical modelling studies to provide insights in the (hydro-)dynamics of regions in the Western Scheldt and Wadden Sea around the sites in these estuaries.
- Climate change affects various processes apart from sea level rise, such as storm surge and wave height. To be able to quantify future hazards, a more comprehensive study might be needed, combining the expected future climate change scenarios by the KNMI

with detailed simulations of the hydrodynamics in the Western Scheldt, Wadden Sea and in front of the North Sea.

- Once more detailed data of the site location and surrounding bed level will become available, a more comprehensive assessment of the risk due to waves can be determined.
- The extreme precipitation is now provided for a nationwide average. Local variability, for instance due to the proximity of the sea, might significantly affect these characteristics. Local data sets or numerical models might be able to highlight possible local effects.
- Further research to quantify the risk of extra-tropical cyclones is required.
- The height of tsunami waves are small compared to wind and swell waves. However, their impact may be much larger, as illustrated in Japan in 2011. Since the probability of occurrence (once per 10^6 years) is in the critical range, it is recommended to investigate the local tsunami impact.

Secondly, at this stage the various risks are assessed separately, which is sufficient at the present stage of site selection. In the design stage, various combinations of risks should be considered simultaneously to quantify the design criteria for the powerplant . For instance, the maximum water levels, due to tides, storms, seiches and waves should be combined to determine the design criteria for the coastal defenses. In the current literature and data study only tides and storm surges are assessed together.

References

De Jong, M.P.C., J. Dekker, and G. Kant (2006), Characteristics of seiches in the Port of Rotterdam during design storm conditions, *Proc. 30th Int. Conf. Coastal Eng.*, Vol. **2**, pp. 1210-1221, 2006.

Deltares (2014a), Statistiek seiches buitenhaven IJmuiden voor ontwerp nieuwe zeesluis, Rapport 1209945-000-HYE-0002 (M.P.C. de Jong, S.P. Reijmerink and M.J.A. Borsboom).

Deltares (2014b), Actualisatie seiches Rotterdam WTI2017 - Waterstandsafhankelijke seiche-waarden, 1209433-006-HYE-0002, 16 december 2014 (S.P. Reijmerink and M.P.C. de Jong).

Deltares (2015a), Inventarisatie van seiches-locaties in Nederland – Verkenning en Plan van Aanpak, 1220039-010-VEB-0001 (M.P.C. de Jong).

Deltares(2015b), Expert-interpretatie seiches buitenhavens Terneuzen, Deltares Memo, 1220093-003-GEO-0002 (M.P.C. de Jong).

Deltares (2015c), Statistische analyse seiches buitenhavens Terneuzen, Deltares Memo, 1220093-003-GEO-0003 (M.P.C. de Jong).

Deltares (2016), Seiches - Invloed op waterkeringen, beperkingen in opwekking en analyse waterstandsmetingen, 1230042-007-ZWS-0001, 17 november 2016 (M.P.C. de Jong, S.P. Reijmerink and J.V.L. Beckers).

Deltares (2017), Seiches – Analyse waterstandsmetingen en invloed opwekkingsmechanismen tijdens extremen, 11200537-009-ZWS-0001, Versie 1, 6 oktober 2017 (S.P. Reijmerink).

De Valk, C.F. en H.W. van den Brink (2023), Update van de statistiek van extreme zeewaterstand en wind op basis van meetgegevens en modelsimulaties. Technisch rapport KNMI TR-406, De Bilt 2023.

HKV (2020), Gebruikershandleiding Hydra-NL, versie 2.8. HKV Lijn in Water report PR4315.10, October 2020 (M. Duits).

IAEA (2011), Meteorological and hydrological hazards in site evaluation for nuclear installations: safety guide/jointly sponsored by the International Atomic Energy Agency and the World Meteorological Organization. — Vienna.

KNMI (2015), KNMI'14-klimaatscenario's voor Nederland; Leidraad voor professionals in klimaatadaptatie, KNMI, De Bilt, 34 pp. Brochure_KNMI14_EN.pdf.

KNMI (2023), KNMI'23-klimaatscenario's voor Nederland, KNMI, De Bilt, KNMI-Publicatie 23.03. https://cdn.knmi.nl/system/ckeditor/attachment_files/data/000/000/357/original/KNMI23_klimaatscenarios_gebruikersrapport_23-03.pdf

STOWA (2019), Neerslagstatistiek en -reeksen voor het waterbeheer 2019, STOWA2019-19. STOWA 2019-19 neerslagstatistieken.pdf and STOWA 2019-19A brochure neerslagstatistieken.pdf.

Taal, M., Meerschaut, Y., Liek, G.J. (2015), Understanding The tides crucial for joint management of the scheldt Estuary. E-proceedings of the 36th IAHR World Congress 28 June – 3 July, 2015, The Hague, the Netherlands 36th IAHR World Congress. https://www.vliz.be/imisdocs/publications/273523.pdf.

Tiessen, M.C.H., J. Groeneweg, R.F. de Graaff, M.P.C. de Jong, P. Siegmund and J.H. Sumihar (2024), Borssele II: site evaluation. Hydro and meteo hazards. Deltares report 11209639-005, January 2024.

A Extreme value distributions wind, water level and wave heights

One of the relevant hazards is an extreme storm, causing strong winds and high water levels and waves. These hydraulic loads may form a serious danger for the dunes and dikes protecting the hinterland and may cause floods. Therefore insight in the extreme values of these hydraulic loads is required. As input for environmental impact studies and to support potential developers of a power plant, marginal statistics of wind speed, water level and wave height are sufficient for now.

The statistical distributions of these parameters are available in tools that have been developed for the safety assessment and design of dunes and dikes in the Netherlands. The probabilistic tools are Riskeer and Hydra-NL. The latter provides hydraulic loads, whereas the first includes descriptions of failure mechanisms and can be used to determine to determined flood probabilities. For the present study we use Hydra-NL.

The wind speed is a stochastic variable in Hydra-NL and the probabilistic distribution of the wind speed is available at several measurement locations. The measurements of the wind have been used to derive the distributions of both wind speed and wind direction. However, the water level and wave height are local variables, being affected by the wind. Within Hydra-NL these hydraulic loads can be determined for arbitrary probabilities of exceedance at output locations in front of the primary sea defense under consideration. For more information about Hydra-NL, see e.g. the User Manual of Hydra-NL (HKV,2020).

A.1 Extreme wind speed

In Hydra-NL the wind statistics of Vlissingen, Cadzand, Hoek van Holland and West-Terschelling are available, apart from other locations that are not relevant for this study. Near Terneuzen there is also a KNMI weather station in Westdorpe, see Figure A.1. Since the measurements at Westdorpe start in 1991 and the measurement series is relatively short compared to e.g. Vlissingen (since 1970), Westdorpe is not considered here. Vlissingen is more sheltered from winds from the North-western sector. As a consequence, the wind speeds will be lower in Vlissingen compared to Cadzand . We prefer to be a bit conservative instead of providing wind speed being to small. Therefore the location Cadzand is considered representative for potential sites Sloegebied and Terneuzen. Station Hoek van Holland is close to Maasvlakte II. At station Hoek van Holland measurements are available since 1971, with a gap from 1981 to 1990. Measurement stations Lauwersoog and Eelde are relatively close to Eemshaven. Lauwersoog is sheltered by Wadden islands and Eelde is a land station, exposed to higher roughness and therefore the wind at both locations is lower than a location at open sea. As can be seen in Figure A.2 West-Terschelling is futher away, but open to winds from the North Sea. Also here we prefer the more conservative wind speed estimates and consider the wind speed at West-Terschelling as representative for Eemshaven.

Figure A.1 Wind measurement locations in southwestern delta

Figure A.2 Wind measurement locations in Wadden Sea area

The directional extreme value distributions for the wind speed, i.e. the probability of exceedance of a wind speed given a directional wind sector, is determined by Caires (2009) based upon measurements at KNMI stations. To derive omnidirectional wind statistics, the directional wind speed statistics need to be multiplied to the statistics of the wind direction. The probability of wind direction is also available in Hydra-NL. For illustration the wind direction statistics in the Western Scheldt is presented in Table A.1. Clearly wind from the south-western quadrant occurs most frequent. For other locations reference is made to the data available in Hydra-NL. Given the probability of occurrence of the wind direction (more specifically 12 directional sectors of 30 degrees) the omni-directional extreme value distribution for the wind speed has been determined.

The extreme value distributions of the wind speed are shown in Table A.2 and Figure A.3 for the three selected measurement locations. The distributions include the effects of uncertainty in the data such as noise and a limited length of a dataset. In Figure A.3 also the wind speed at Vlissingen is presented, to show that the wind speed at Cadzand is higher than at Vlissingen, approximately 2 m/s.

Additionally, with the directional extreme value distribution of wind speed and the probability of occurrence of wind direction a wind rose can be composed, if requested in a next stage of the hazards assessment.

Table A.1 Probability of occurrence of wind direction in the Western Scheldt.

Direction	Probability	Direction	Probability
30	0.042	210	0.162
60	0.065	240	0.144
90	0.087	270	0.099
120	0.061	300	0.070
150	0.064	330	0.048
180	0.117	360	0.041

Table A.2 The omni-directional wind speed [m/s] being exceeded for various return periods.

Return period [years]	Cadzand	Hoek van Holland	West-Terschelling
10	25.5	24.5	25.8
100	30.0	28.6	29.9
1000	34.6	32.7	34.0
10.000	39.3	36.8	38.1
100.000	44.1	41.1	42.3
1.000.000	49.1	45.3	46.8

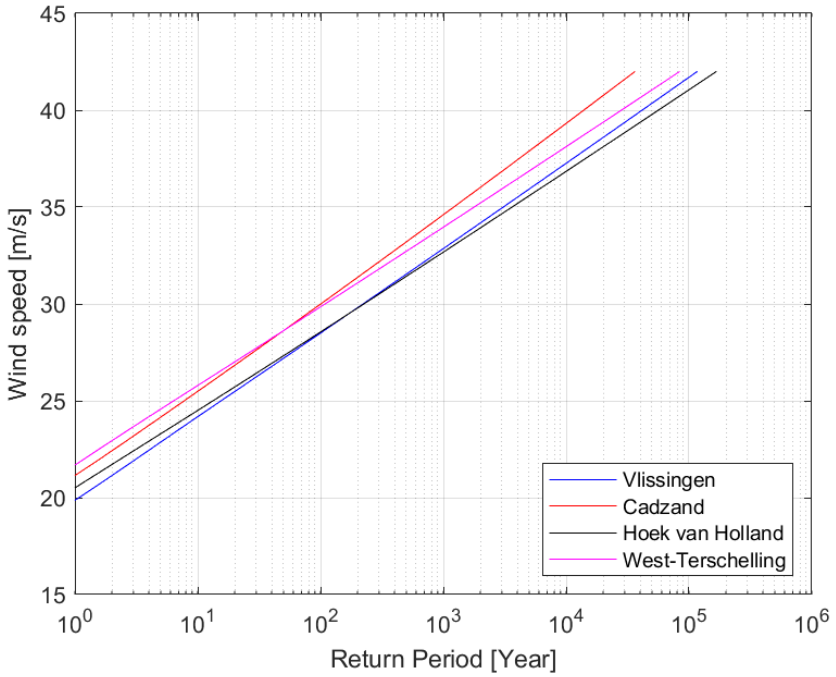

Figure A.3 Probability of exceedance curves for the wind speed at Vlissingen, Cadzand, Hoek van Holland and West-Terschelling, including statistical uncertainties.

A.2 Extreme wave height

Whereas the extreme value distribution for wind has been determined from measurement data and forms input for Hydra-NL, the extreme value distribution for local wave height and water level are output of Hydra-NL. Wind is here the driving factor. Output locations have been selected for the four potential locations, that are available within the Hydra-NL database. The study for Borssele (Deltares, 2023) showed a strong spatial variability in significant wave height, due to the strong spatial variation in both bed height and orientation of the dike. This is also observed for the locations considered in the present study. Table A.3 shows the range of significant wave heights in front of the potential NPP locations for the return periods 10, 10.000 and 1.000.000 years. Especially for Maasvlakte and Terneuzen the spatial variation of wave height is large. On either side of Eemshaven the spatial variation of wave height is limited . The frequency exceedance curves of the significant wave height at the output locations is presented in Figure A-4 to Figure A-6. Since Sloehaven is seaward of the primary sea defence near Vlissingen, Hydra-NL does not contain output locations in front of the two potential NPP locations. In Figure A-7 the closest two locations on the eastern and western side, as well as the location at the entrance of Sloehaven are presented. The variation in wave height at these three locations is large and it is questionable whether the wave heights at these locations are representative for the waves reaching the two plant locations. A further study about the propagation of waves towards the plant locations is required to get a more accurate estimate of the wave height.

The significant wave heights at all locations are presented in Table A.3.

Table A.3 The range of significant wave heights [m] in front of the potential NPP locations for 3 return periods [years].

		10	10000	1000000
Eemshaven	East	1.8 - 1.9	3.5 - 3.7	4.8 - 5.0
	West	1.2 - 1.3	2.3 - 2.4	3.1 - 3.3
Maasvlakte II		4.1 – 5.5	7.6 – 10.0	9.5- 11.9
Terneuzen		1.0 - 1.4	2.0 - 2.6	2.7 - 3.5
Sloegebied	East	1.0	2.0	2.8
	Entrance	2.5	4.0	4.8
	West	1.5	2.3	2.7

When a more precise site location is determined (and potentially even changes in the bed height in front of the potential NPP locations, because the bed topography in the underlying wave computations is at least 15 years old), a more detailed assessment can be made regarding the occurrence of a significant wave height at the site location.

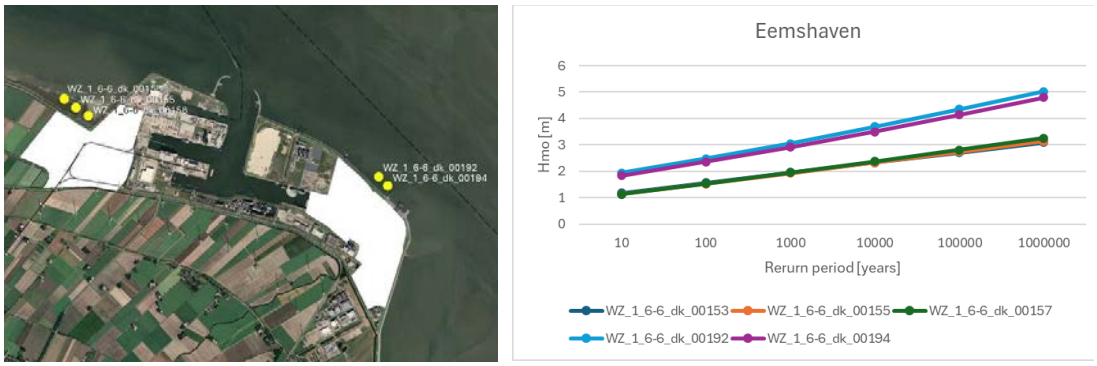

Figure A-4 Probability of exceedance curves for the significant wave height at five locations near Eemshaven (split into eastern and western part).

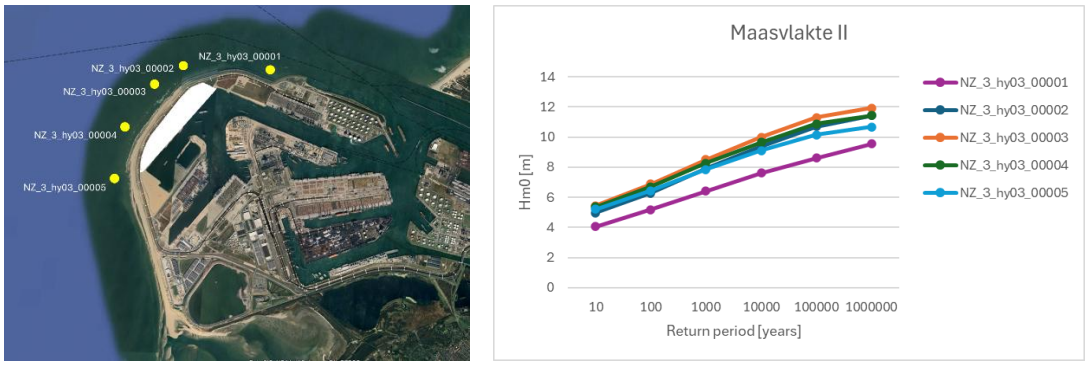

Figure A-5 Probability of exceedance curves for the significant wave height at five locations near Maasvlakte II.

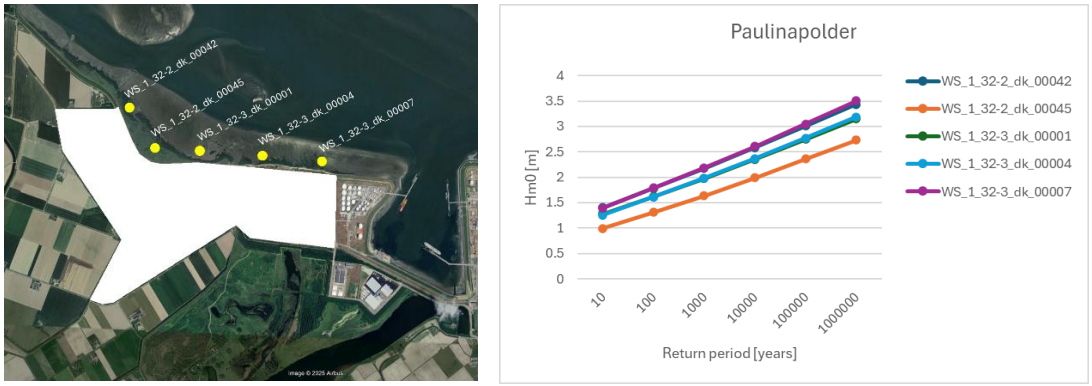

Figure A-6 Probability of exceedance curves for the significant wave height at five locations near Terneuzen.

Figure A-7 The three output locations closest to the two potential NPP locations at the Sloegebied, that are available in Hydra-NL.

A.3 Extreme water level

For various recurrence periods the water levels can be determined with Hydra-NL at the same output locations considered for the wave heights. For wave heights the spatial variation is large. The water level is almost insensitive to bed level and dike orientation. Therefore the spatial variation is small. In Table A.4 the water levels for the return periods from 10 to 1.000.000 years are presented at the four plant locations. The spatial variation over the output locations being considered is given in brackets. The variation is in the order of centimeters. For Sloehaven only one output location is considered on either side of the entrance. Therefore, no variation is given. The difference between eastern and western side of the harbours of Sloehaven and Eemshaven is in the order of 1-2 dm. Therefore water levels at both sides are presented.

Table A.4 The water level being exceeded for various return periods [m + NAP] at the indicated output location indicated in Figures A-4 to A.7. In between brackets the variation over the output locations being considered.

Return period [years]	**Terneuzen** WS_1_32-3_dk_00001	**Maas-vlakte-II** NZ_3_hy03_00003	**Sloehaven West** WS_1_29-3_dk_00002	**Sloehaven East** WS_1_30-4_dk_00006	**Eemshaven West** WZ_1_6-6_dk_00155	**Eemshaven East** WZ_1_6-6_dk_00192
10	4.10 (±0.03)	3.06 (±0.01)	3.90	3.99	3.65 (±0.01)	3.73 (±0.01)
100	4.71 (±0.04)	3.69 (±0.01)	4.48	4.58	4.39 (±0.01)	4.48 (±0.01)
1000	5.34 (±0.04)	4.38 (±0.01)	5.07	5.18	5.07 (±0.02)	5.18 (±0.02)
10.000	5.99 (±0.04)	5.15 (±0.01)	5.67	5.81	5.73 (±0.02)	5.86 (±0.02)
100.000	6.68 (±0.05)	6.01 (±0.01)	6.32	6.48	6.40 (±0.02)	6.54 (±0.02)
1.000.000	7.42 (±0.06)	6.88 (±0.01)	7.00	7.18	7.07 (±0.02)	7.23 (±0.02)

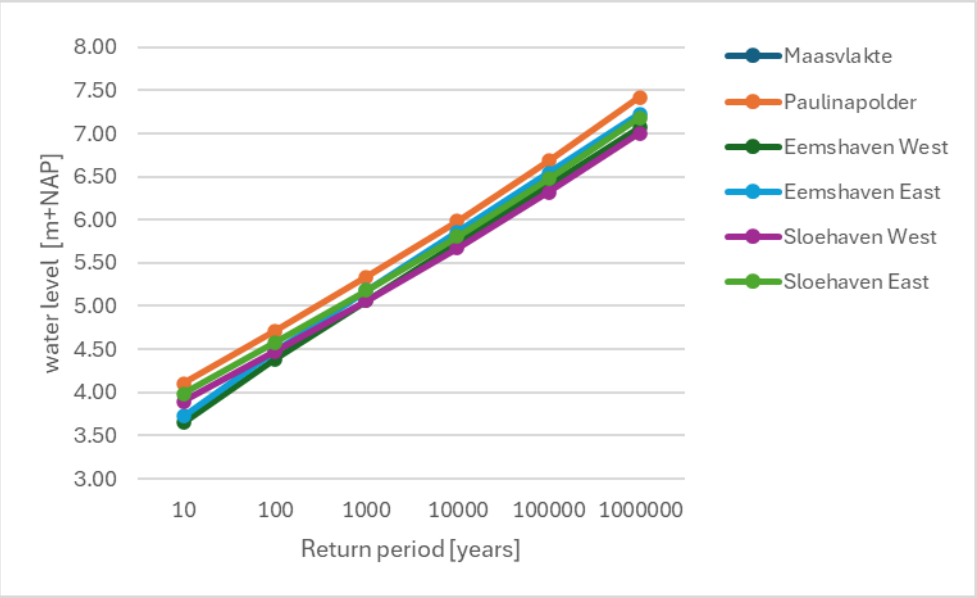

Figure A.8 Probability of exceedance curves for the water levels (in m+NAP) at the output locations in Table A.4).

A.4 References

Caires, S. (2009). Extreme wind statistics for the Hydraulic Boundary Conditions for the Dutch primary water defences. SBW-Belastingen: Phase 2 of subproject "Wind Modelling". Deltares report 1200264-005, September 2009.

Dillingh, D., L. de Haan, R. Helmers, G.P. Können, J. van Malde (1993). De basispeilen langs de Nederlandse kust; statistisch onderzoek, Rijkswaterstaat, Dienst Getijdenwateren /RIKZ, Report DGW-93,023.

Tiessen, M.C.H., J. Groeneweg, R.F. de Graaff, M.P.C. de Jong, P. Siegmund and J.H. Sumihar (2024). Borssele II: site evaluation. Hydro and meteo hazards. Deltares report 11209639-005, January 2024.

De Valk, C.F. en H.W. van den Brink (2023). Update van de statistiek van extreme zeewaterstand en wind op basis van meetgegevens en modelsimulaties. Technisch rapport KNMI TR-406, De Bilt 2023.

B Post-tropical cyclones and extreme precipitation in the Netherlands

B.1 Introduction

This appendix provides a concise overview of current literature on several types of extreme weather in the present and future climate of the Netherlands. The focus is on post-tropical cyclones and on extreme precipitation. In addition, some information on hail, snow, and thunderstorms is provided.

B.2 Post-tropical cyclones in the Netherlands

B.2.1 Tropical and post-tropical cyclones

Tropical cyclones, or hurricanes, are extremely powerful storms that can develop over areas with warm sea water (> 26.5°C). Their energy source is the heat stored in seawater. By means of surface evaporation and subsequent condensation of the water vapor in the atmosphere by deep vertical motions, the heat of seawater is transferred to the atmosphere and finally converted into kinetic energy of tropical cyclones. The condensation leads to large amounts of rain fall.

Some tropical cyclones move northward along the US East Coast, losing their tropical character and turning into an extra-tropical storm. At the height of Newfoundland these post-tropical cyclones are carried by the jet stream towards Europe, and on the way they can regain strength under favorable conditions.

In a warming climate three different mechanisms might contribute to more and more intense post-tropical cyclones in Europe (Haarsma, 2021):

1. The strength of tropical cyclones is expected to increase. Stronger tropical cyclones will have a larger chance to survive over the cooler midlatitude sea water before entering Europe.
2. Areas with high water temperatures are moving closer to Europe.
3. In the present climate, the north-eastern part of the tropical Atlantic is too cool for the genesis of tropical cyclones, but will become warmer than 26.5°C in a warmer climate.

Tropical cyclones that originate in the middle and western part of the tropical Atlantic, usually follow a C-shape curve along the US east coast before entering Europe. On the contrary tropical cyclones that originate in the north-eastern part of the tropical Atlantic can, by traveling in north-easterly direction, take a shortcut to Europe.

B.2.2 Observations

During the hurricane season (June-November) almost 9% of all severe storms in the North Sea (> 25 m/s) are originally hurricanes (Sainsbury et al., 2020). The average strength of these post-tropical cyclones is also larger than that of other storms. A study on European cyclones with tropical origin in reanalysis data revealed that in the period 1979-2013 53 hurricanes have entered the European area (Dekker 2018; KNMI, 2019). A very few of them still had hurricane strength when they hit the western part of the British Isles. The Netherlands has never been hit by a post-tropical cyclone with hurricane force (Beaufort 12 with wind speeds exceeding 32.6 m/s). From the observational data the conclusion is therefore that the risk of the Netherlands being hit by a post-tropical cyclone with Beaufort 12 is negligible.

Europe was hit in October 2017 by hurricane Ophelia (Rantanen et al., 2020) that originated as the most northern eastward major (category 3) hurricane close to the Azores since the start of the observations and traveled in a straight line toward Ireland. It arrived there, after re-intensification, as a category 1 hurricane. It was partly caused by the locally very warm sea water temperatures (KNMI, 2019). Ophelia can be considered as a show case for what might become more common in a warmer climate (Haarsma, 2021). The British Isles are not necessarily a barrier: according to a model simulation, Ophelia could just as well have squeezed through the Straits of Calais to reach with hurricane force winds the Dutch coast (De Vries et al., 2018). The path of Ophelia was caused by the large-scale atmospheric circulation, and a slightly more easterly path is considered as a realistic possibility. In October 2024 post-tropical cyclone Kirk caused significant damage in portions of Western Europe. In early predictions the cyclone track passed the Netherlands, but in later predictions and in reality the cyclone made landfall in south-west France.

B.2.3 Future climate

In a warmer climate the strength of hurricanes is expected to increase (Knutson et al., 2020). Haarsma et al. (2013) used a very high resolution global climate model (~25 km grid size) with prescribed sea surface temperatures to show that greenhouse warming enhances the occurrence of hurricane-force (wind speeds larger than 32.6 m/s) storms over western Europe during early autumn (August–October), the majority of which originate as a tropical cyclone. Summed over Norway, the North Sea, and the Gulf of Biscay the number of hurricane force storms increases from 2 to 13 over the 21st century. Over the North Sea the season of highest occurrence of severe storms (say Beaufort 11-12, i.e. wind speeds larger than 28.4 m/s) shifts from winter to autumn. In a more detailed analysis with the same model and resolution, Baatsen et al. (2015) found for a moderate warming scenario (RCP4.5) a major increase in the number of Autumn storms (Beaufort 11-12) originating in the tropical Atlantic: from 15 in the present (2002-2006) to 23 in the near future (2030-2034) and 37 in future (2094-2098) climate simulation (Figure-appendix B-1).

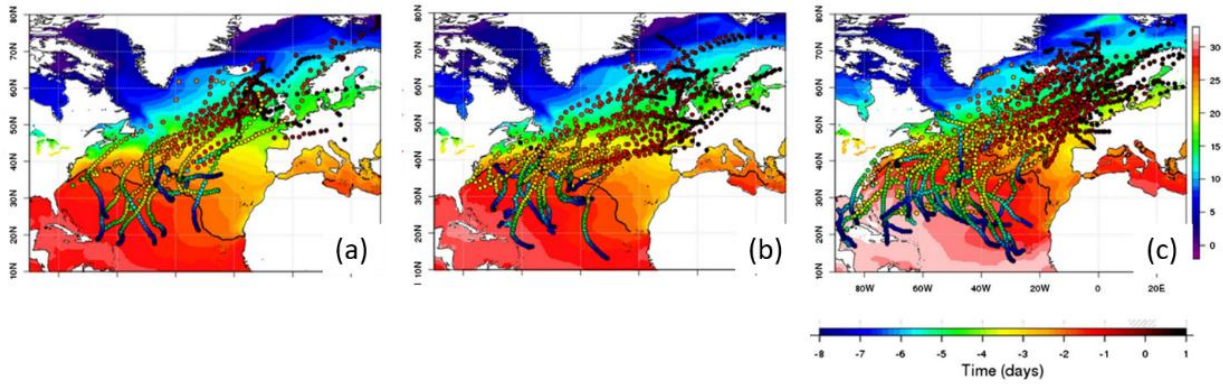

Figure-appendix B-1 Tracks for present (a), near future (b) and future (c) cyclones. The panels show the storm tracks and August-October mean sea surface temperatures (°C) for the respective periods, the thick black line is the 26 °C isotherm. The color scale of the circles indicates the duration in days before the moment that 11 Beaufort wind speed was reached. Source and more details: Baatsen et al., 2015.

Each simulation for present, near-future and future climate consists of a 6-member ensemble spanning 5 years, resulting in a 30 year dataset. The model simulated a wind speed for the North Sea of 37 m/s during a 30-year simulation that according to extreme value statistics would occur only once in the 20.000 year for the present climate (KNMI, 2019). Analysis of a simulation with another climate model, that of the Geophysical Fluid Dynamics Laboratory,

has confirmed the increased risk of Western Europe to be hit by extra-tropical storm that origin from hurricanes (Liu et al. 2017). Further research with high-resolution climate models is required to further investigate the potentially high windstorm risk for Europe in the future of remnants of tropical cyclones (Haarsma, 2021).

Baatsen et al. (2015) also analyzed the dynamics of hurricanes that reach Europe. The mechanism for their intensification is the combination of the release of latent heat caused by heavy precipitation, which is the thriving force of hurricanes, and baroclinic instability, which is the mechanism for traditional mid-latitude storms. On their way to Europe the hurricanes transform into extra-tropical storms and expand in size. After an initial weakening during this transformation when they enter the cooler waters of the Atlantic Ocean, they re-intensify in a later stage and regain hurricane force on entering the European coast. The storms of tropical origin also led to so-called atmospheric rivers with a large amount of water vapor, that will influence the future European climate accompanied by a higher potential for floods.

B.3 Extreme precipitation

B.3.1 Observations

Information of (extreme) rain in the Netherlands is provided by STOWA (2019) as the amount of rain at a given rainfall duration (two hours to eight days), which is exceeded with a certain frequency (twice a year to once a 1000 years) (Figure-appendix B-2). The information applies to any location in the Netherlands. For example, 50 mm rain in two days occurs on average once per 2 years, and 100 mm in two days once per 50 years. A heavy shower, defined by KNMI as 25 mm or more in one hour, occurs about once per 5 years.

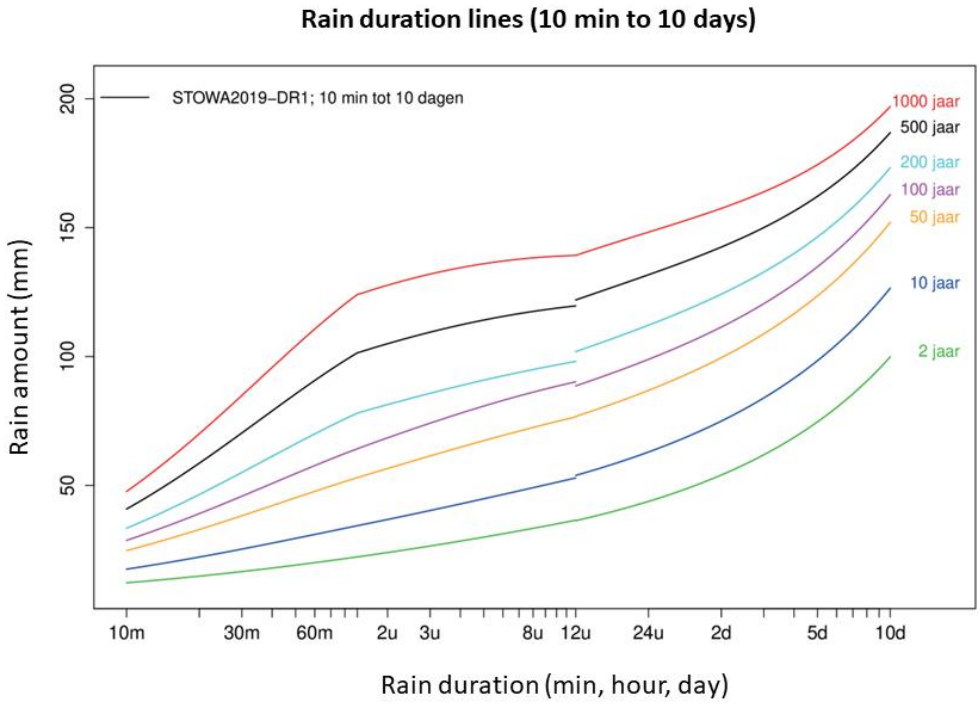

Figure-appendix B-2 Rain duration lines based on precipitation observations in the Netherlands for the whole year. Source: STOWA (2019).

The average amount of precipitation per year in the Netherlands increased by 9% between 1961-1990 and 1991-2020. If for each 30-year period the daily precipitations are ranked from highest to the lowest amount, for almost all ranked days the precipitation increase is also about 9%, except for the extremely wet days, for which the increase is up to 15% (KNMI,

2022). The number of very wet days – with at least 10 mm of precipitation in winter and at least 20 mm in summer – increased between 1961-1990 and 1991-2020 by about a quarter: from 4.3 to 5.3 days per winter and from 1.5 to 1.9 days per summer (KNMI, 2021). Between these periods the annual maximum precipitation per day in the Netherlands increased from 33 to 37 mm, and in De Bilt the annual maximum precipitation per hour increased from 15 to 19 mm.

B.3.2 Future climate

In a warmer climate, the atmosphere contains more water vapor. As a result, more precipitation falls from a shower. More water vapor in the atmosphere also means that more heat of condensation is released, so that the air in showers rises faster and rains out faster. On the other hand, due to the condensation the air at higher altitudes warms more than air near the Earth's surface. This makes the atmosphere more stable, which slows down the vertical motions in the showers. The increase in condensation heat will probably have a greater effect and, therefore, extreme showers are expected to occur more often in the future.

In the KNMI'23 climate scenario's precipitation extremes increase throughout the year in all scenario's, except in the Ld-scenario (low emissions, dry variant) in winter. Such precipitation extremes can be caused by two meteorological phenomena: fronts associated with depressions, or rain showers caused by vertical instability of the atmosphere. Fronts are typical in winter, whereas showers are typical in summer, but often a combination of both occurs. While fronts are well resolved in the climate models used for developing the scenarios, rain showers, which cause the extreme precipitation peaks in summer, are not. Consequently, the change in precipitation extremes for a particular summer scenario is quite uncertain. In the KNMI'23 scenario's in winter the 10-day amount exceeded once in 10 years changes, relative to the refence period 1991-2020, by -2% to +2% around 2050 and -2% to +15% around 2100, positive changes being an increase and negative changes a decrease. In summer the daily amount exceeded once in 10 years increases by +4% to +11% around 2050 and +4% to +31% around 2100. The maximum hourly amount per year increases by +4 to +11% around 2050 and +4 to +31% by 2100.

B.4 Hail, snow, and thunderstorms

B.4.1 Hail

Due to the lack of long, high-quality measurements, little is known about possible trends in the frequency and intensity of hail. Information about hail in the future is only very limited. Because there is more water vapor in the atmosphere and vertical motions intensify, the largest hail stones are likely to become even larger. Regional climate models have been used to determine the frequency of hail with a diameter of 50 mm or more for Europe (Rädler et al., 2019). In the Netherlands, the frequency is highest in the southeast, about once every 15 years. At the end of this century, this frequency will increase, in case of an average global warming of 2 degrees, to about once every 10 to 12 years.

B.4.2 Snow

The number of days with snowfall in the Netherlands increases from the south-west to the north-east, from about 14 days per year in Zeeland (average for 2003-2020) to 24 days in the north-east. The KNMI'23 scenario's do not provide information for snowfall in the future, but given the future warming of the Netherlands the frequency of snowfall is expected to decrease. As a relative proxy for the frequency of snowfall one might use the frequency of frost days, on which the minimum temperature is below 0°C. Around 2050 the frequency of frost days in De Bilt is expected to be decreased by 26% to 44% relative to the reference period 1991-2020 (KNMI, 2023).

B.4.3 Thunderstorms

Thunderstorms are implicitly discussed in the section on extreme precipitation. Wind gusts and downburst that accompany thunderstorms can become stronger in the future (KNMI'21). Future changes in the frequency of lightning are uncertain.

B.5 References

Baatsen et al., 2015: Severe Autumn storms in future Western Europe with a warmer Atlantic Ocean, Clim Dyn 45:949–964. http://doi.org/10.1007/s00382-014-2329-8.

CLO, 2019: Neerslagextremen in Nederland, 1910-2019. https://www.clo.nl/indicatoren/nl0590-neerslag-extremen.

Dekker et al., 2018: Characteristics and development of European cyclones with tropical origin in reanalysis data, Clim Dyn 50:445–455. https://doi.org/10.1007/s00382-017-3619-8.

De Vries et al., 2018: Als orkaan Ophelia Nederland had bereikt. Meteorologica, 27, 4-8. https://www.nvbm.nl/meteorologica/archief/2010-2019/2018/september-2018.

Haarsma et al., 2013: More hurricanes to hit Western Europe due to global warming. Geophys. Res. Let., 40, 1783-1788. https://doi.org/10.1002/grl.50360.

Haarsma, R., 2021: European Windstorm Risk of Post-Tropical Cyclones and the Impact of Climate Change, Geophys. Res. Let., 48. https://doi.org/10.1029/2020GL091483.

KNMI, 2015: KNMI'14 climate scenarios for the Netherlands; A guide for professionals in climate adaptation, KNMI, De Bilt, The Netherlands, 34 pp. https://cdn.knmi.nl/system/data_center_publications/files/000/070/807/original/Brochure_KNMI14_EN_2015.pdf?1653079346 .

KNMI, 2019: Climatology of the PALLAS site near Petten (not publicly available).

KNMI, 2021: KNMI Klimaatsignaal'21: hoe het klimaat in Nederland snel verandert, KNMI, De Bilt, 72 pp. https://cdn.knmi.nl/knmi/asc/klimaatsignaal21/KNMI_Klimaatsignaal21.pdf .

KNMI, 2022: Als het regent, valt er 9% meer regen dan 50 jaar geleden, KNMI klimaatbericht, https://www.knmi.nl/over-het-knmi/nieuws/als-het-regent-valt-er-9-meer-regen-dan-50-jaar-geleden .

KNMI, 2023: KNMI'23-klimaatscenario's voor Nederland, KNMI, De Bilt, KNMI-Publicatie 23.03. https://cdn.knmi.nl/system/ckeditor/attachment_files/data/000/000/357/original/KNMI23_klimaatscenarios_gebruikersrapport_23-03.pdf

Knutson et al., 2020: Tropical Cyclones and Climate Change Assessment: Part II: Projected Response to Anthropogenic Warming. BAMS. 101, E303-E322. https://doi.org/10.1175/BAMS-D-18-0194.1 .

Liu et al., 2017: The present-day simulation and twenty-first-century projection of the climatology of extratropical transition in the North Atlantic. J. Clim., 30(8), 2739-2756. https://doi.org/10.1175/JCLI-D-16-0352.1 .

Rädler et al., 2019: Frequency of severe thunderstorms across Europe expected to increase in the 21st century due to rising instability. npj Clim Atmos Sci 2, 30. https://doi.org/10.1038/s41612-019-0083-7 .

Rantanen et al., 2020: The extratropical transition of Hurricane Ophelia (2017) as diagnosed with a generalized omega equation and vorticity equation. Tellus, Series A: Dynamic Meteorology and Oceanography, 72(1), 1–26. https://doi.org/10.1080/16000870.2020.1721215 .

Sainsbury et al., 2020: How important are post-tropical cy1clones for European windstorm risk? Geophysical Research Letters, 47, e2020GL089853. https://doi.org/10.1029/2020GL089853 .

STOWA, 2019: Neerslagstatistiek en -reeksen voor het waterbeheer 2019, STOWA2019-19. STOWA 2019-19 neerslagstatistieken.pdf and STOWA 2019-19A brochure neerslagstatistieken.pdf.

C Tsunami risks

C.1 Introduction

Tsunamis are waves propagating in the sea as a result of a sudden vertical displacement of the water column due to, for example, a submarine earthquake or landslide. Offshore, tsunamis can have wavelengths of up to a few 100 km's and wave amplitudes of usually less than 1 m. When tsunami waves approach the coast, the propagation speed decreases and the amplitude increases, potentially leading to coastal inundation.

The occurrence of destructive tsunamis in the North Sea and along the Dutch coast is very unlikely since there are no major tsunami sources (esp. earthquakes or landslides) present in the North Sea. Moreover, the shallow waters of the North Sea cause strong dissipation of a tsunami coming from the Atlantic Ocean or Norwegian Sea, which will therefore lose most of its energy before reaching the Dutch coast (e.g. DEFRA, 2005, Chacón-Barrantes et al., 2013, Bork et al., 2007). In absence of detailed studies on tsunami risks, this section summarizes the probability of tsunami occurrence and estimated maximum tsunami wave heights at the Dutch coast, based on a literature review combined with expert judgement.

C.2 Potential sources for tsunami's at Duch coast

Potential sources of tsunamis reaching the Dutch coast are submarine earthquakes at (distant) subduction zones or at (local) fault zones, submarine landslides, erupting or collapsing volcanoes, meteorites, or fast-propagating storm fronts along the coast causing meteotsunamis. Each of these potential sources are discussed briefly below.

C.2.1 Tsunamis due to submarine earthquakes at (remote) subduction zones

Most tsunamis in the world are caused by sudden vertical motions in the earth's crust at so-called subduction zones, where one tectonic plate dips under another tectonic plate with lower density. These subduction zones, and therefore the origin of tsunamis, are mostly located in the Pacific Ocean ('Ring of Fire', see Figure-appendix C-1).

Subduction zones in the Atlantic Ocean are less extensive and more passive than the ones in the Pacific Ocean. The only known significant tsunami that occurred in the Atlantic Ocean due to plate tectonics was in 1755 AD. This tsunami was the result of Mw 8.5 submarine earthquake with its epicenter about 200 km to the west of Portugal (Sousa et al., 1992). According to historic evidence published in DEFRA (2005), it is unlikely that the Lisbon 1755 tsunami has led to a significant tsunami at the Dutch coast. There is a probability that tsunamis will be triggered at the same subduction zone in the future. However, it is expected that these will be less severe than in 1755 AD (Baptista et al., 2003).

The same accounts for a tsunami generated due to a submarine earthquake in the Caribbean. According to DEFRA (2005) it is likely that an extreme submarine earthquake event at the Caribbean subduction zone has already happened, but that this event did not lead to a significant tsunami reaching the coasts of northwestern Europe.

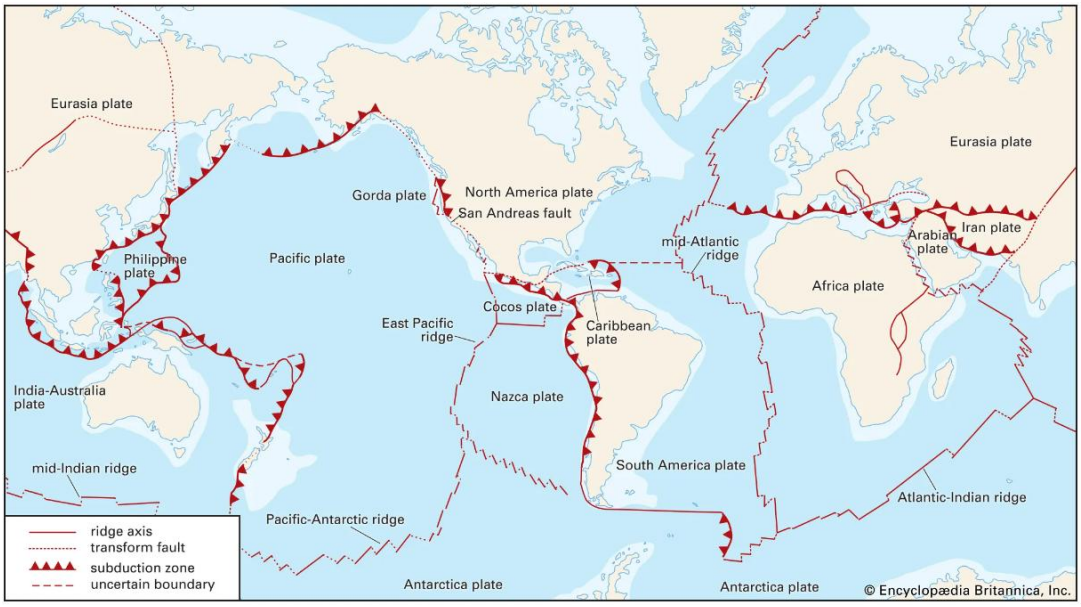

Figure-appendix C-1 Subductions zones in the world (source: www.britannica.com/science/subduction-zone).

C.2.2 Tsunamis due to submarine earthquakes at fault zones in the Southern North Sea

In DEFRA (2005) it is stated that the occurrence of a 6.5 M_w earthquake in the North Sea, which is within the lower range for tsunamigenic earthquakes, cannot be ruled-out. In the North Sea, a few submarine earthquakes have been observed in the past, namely a 5.7 M_w earthquake in 1927 with its epicenter in the northern part of the North Sea (Viking Graben), and a 6.1 M_w earthquake in 1931 with its epicenter in the southern part of the North Sea (Sole Pit Basin or Dogger Bank). According to DEFRA (2005) there is no evidence of significant tsunami waves reaching the UK or Dutch coasts as a result of these two earthquakes.

C.2.3 Tsunamis due to submarine landslides

After submarine earthquakes, submarine landslides are the second most frequent tsunami source worldwide. Submarine landslides are however much more diverse in nature and very difficult to predict (Løvholt et al., 2020). Near their source, landslide-generated tsunamis may result in higher tsunami wave heights than seismically generated tsunamis, but will usually lose energy quickly due to wave energy dissipation and/or divergence, and rarely affect distant coasts (NOAA, 2023).

For the Dutch coast the most likely source of a landslide tsunami is off the coast of Norway (Figure-appendix C-2). According to sediment deposits along the coasts of Norway, Faeroes Islands, Shetland Islands and in the area of the Dogger Bank, it is believed that a large tsunami occurred about 8200 years ago in the northern part of the North Sea, the so-called Storegga Slide (Bondevik et al., 2005; Gaffney et al., 2020). When this tsunami wave propagated into the central and southern part of the North Sea, it is likely to have reached the prehistoric Dutch coast with maximum wave heights of about 1.0 m in the north to about 0.5 m in the south (Figure-appendix C-3, Twigt and Blaas, 2007). Similar simulations were made by Lehfeldt et al. (2007), indicating similar results. Other landslides may occur in the future in the same area, but probably with smaller volumes as compared to the Storegga Slide (DEFRA, 2005) and therefore with smaller expected typical tsunami wave heights.

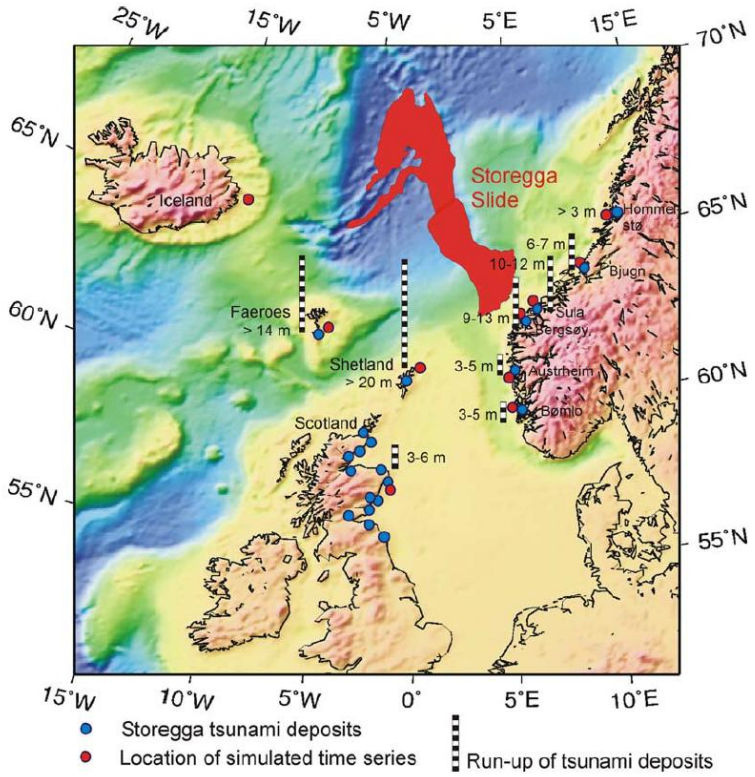

Figure-appendix C-2 Map of the Storegga Slide, run-up heights (bars) and study locations (dots) from Bondevik et al., 2005.

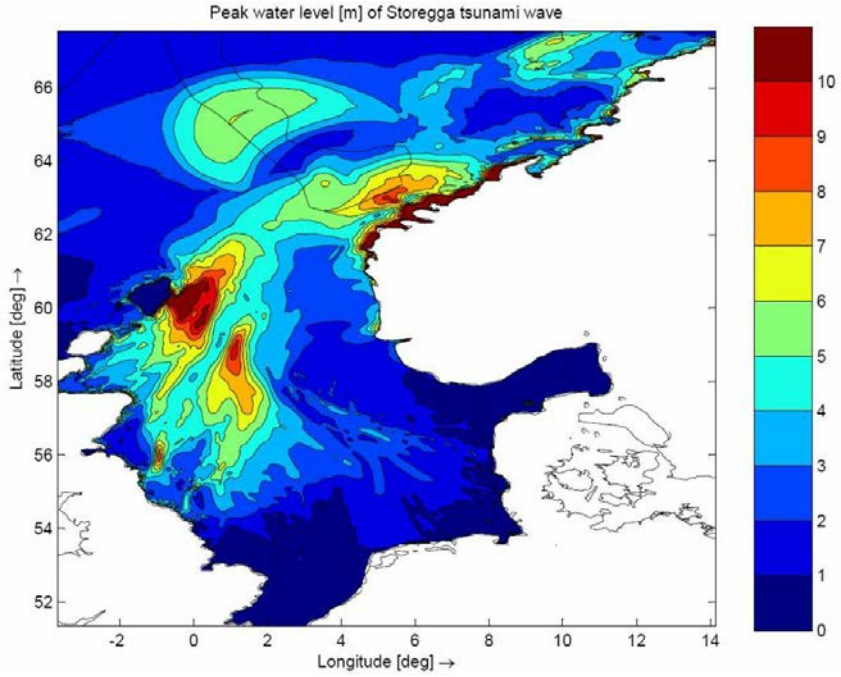

Figure-appendix C-3 Computed peak water levels as a result of the Storegga Slide, from Twigt and Blaas, 2007.

C.2.4 Tsunamis due to erupting or collapsing volcanoes

Ocean-based volcanoes that erupt or collapse are a potential trigger for tsunamis. It has been suggested by Ward and Day (2001) that a landslide on the flank of La Palma, one of the Canary Islands, will result in a potentially very high tsunami in the North Atlantic Ocean.

Nevertheless, numerical model simulations by Abadie et al. (2020) show that a tsunami originating from La Palma will not be able to propagate into the North Sea (Figure-appendix C-4). Other potential sources of volcanogenic tsunamis are Cape Verde or along the Mid-Atlantic Ridge, however, it is very unlikely that such events will result in significant tsunami wave heights at the North Sea coasts (DEFRA 2005).

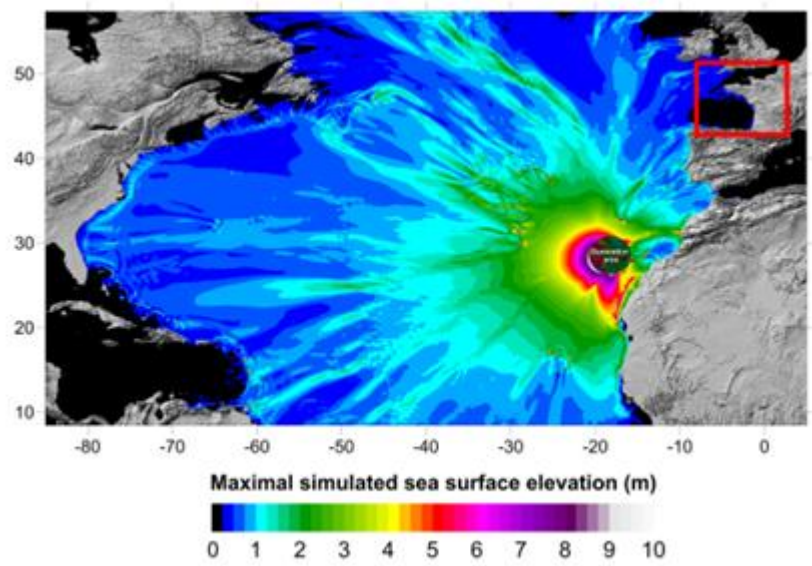

Figure-appendix C-4 Maximum wave height as a result of a hypothetical tsunami due to flank collapse at La Palma (from: Abadie et al., 2020).

C.2.5 Tsunamis due to meteorite impacts

The probability of a significant tsunami resulting from a meteorite striking the Atlantic Ocean or bordering seas is extremely low. Paine (1999) argues that only meteorites with a diameter of 200 m or more will trigger tsunamis. According to the diagram in Figure-appendix C-5 the probability of a 200 m wide meteorite hitting the earth has a recurrence interval of at least 10.000 years, obviously with a very large degree of uncertainty. The probability of such a meteorite hitting the North Atlantic Ocean and resulting in a tsunami that will affect the Dutch coast, will be even lower.

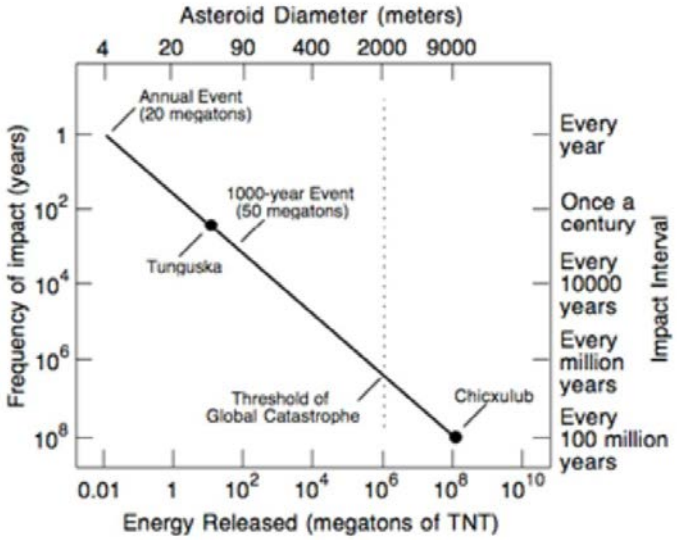

Figure-appendix C-5 Relationship between the size of a meteorite and the frequency of occurrence (from: geology.com/articles/near-earth-asteroids.shtml)

C.2.6 Tsunamis due to fast moving storm fronts

Fast moving convective storm fronts, leading to rapid changes of surface pressure, can result in long waves propagating along the coast (De Jong, 2004; and Section 2.5.1). These meteo-induced long waves are also referred to as meteotsunamis.

Meteotsunamis are probably the most likely source of tsunamis at the Dutch coast. The most recent meteotsunami at the Dutch coast occurred on May 29, 2017 (Figure-appendix C-6), with a measured 0.9 m wave height along the coast and an estimated wave run-up height of 2 m on the beach (Sibley et al., 2021). In Frère et al. (2014) a meteotsunami in 2011 is presented, propagating from the south of Portugal, along the French coast and into the English Channel. According to the Royal Dutch Meteorological Institute (KNMI), meteotsunamis occur several times per year but are often unnoticed[3]. Another significant meteotsunami affecting the Dutch Coast (and Lake IJssel) occurred on July 11th, 1984. According to KNMI, the intensity of meteotsunamis may increase due to climate change.

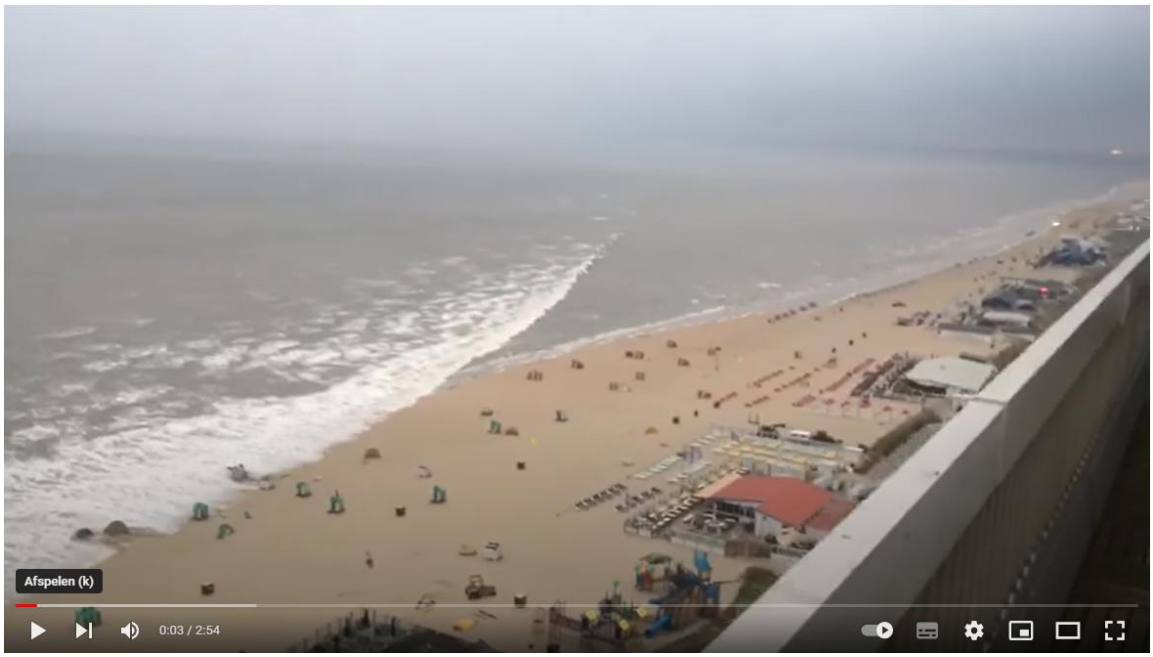

Figure-appendix C-6 Video still from the meteotsunami at the Dutch coast on May 29, 2017 (source: https://www.youtube.com/watch?v=CjQk_xt_WU0).

C.2.7 Estimates of maximum tsunami height and recurrence intervals

As mentioned in the introduction of this section, tsunami wave heights in the southern part of the North Sea are limited, which is partly related to the shallow water depths and resulting energy dissipation. Bork et al. (2007) illustrated this effect by making simulations with realistic water depths in the North Sea and assuming a fictitious uniform deep water of 500 m in a separate calculation. The left panel of Figure C-7 shows that the tsunami wave heights reaching the North Sea are limited when considering realistic water depths. The right panel of that figure shows that if the North Sea would have been much deeper (500 m in this case, although the precise value is not critical for making this point), much higher tsunami wave heights would occur in this area. However, this will not be the case in reality.

[3] https://www.knmi.nl/kennis-en-datacentrum/achtergrond/meteo-tsunami-treft-nederlandse-kust)

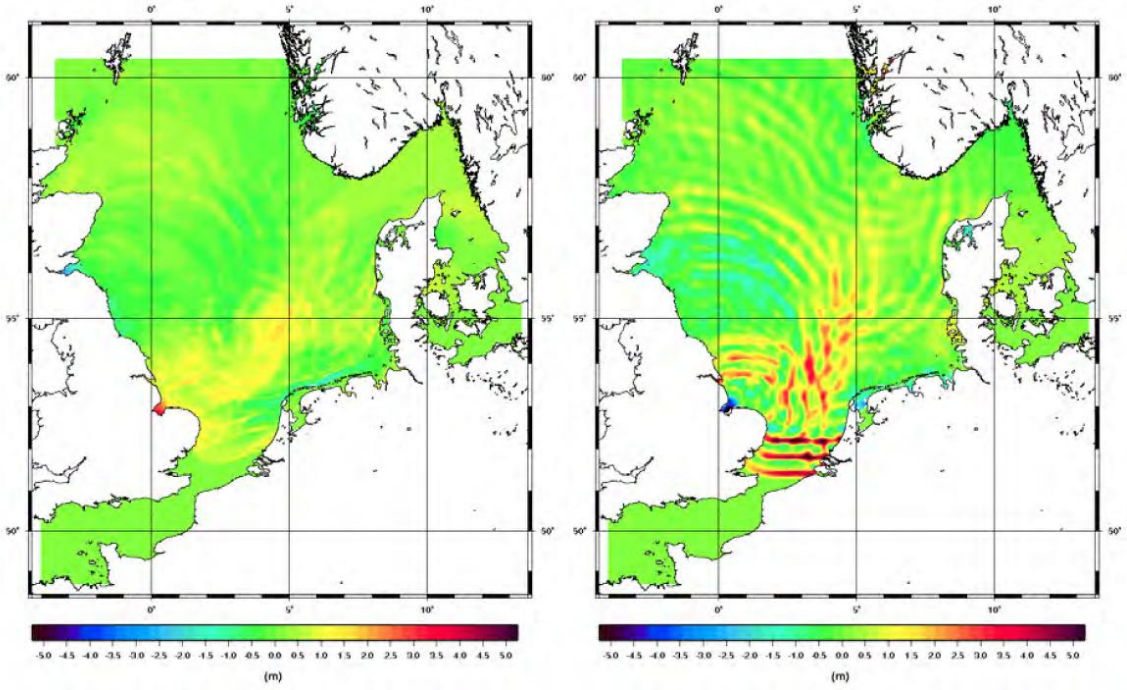

Figure-appendix C-7 Results of tsunami model simulations in the North Sea assuming realistic water depths (left) and uniform deep water of 500m (right) (from: Bork et al., 2007)

Similar to tsunami waves approaching the Dutch coast from the north, tsunami waves propagating through the British Channel will also be largely attenuated due to the limited width and depths of the Channel (e.g. Chacón-Barrantes et al., 2013).

On the basis of the literature review combined with expert judgement, the table below summarizes indicative values of the maximum possible tsunami wave heights along the Dutch coast, and their estimated probability of occurrence for the various tsunami sources.

Table-appendix C-1 Maximum possible tsunami wave heights at the Dutch coast, and its estimated probability of occurrence for various tsunami sources.

Tsunami source	Indications of upper estimates of tsunami wave heights along the Dutch Coast	Very rough indication of probability of associated return periods [years]	Literature reference
Submarine earthquakes at subduction zones	insignificant	not relevant	DEFRA, 2005
Submarine earthquakes at fault zones in the North Sea	2 m 0.75 m 0.50 m	100.000 5.000 500	Van Malde, 1990 Bijl, 1993
Submarine landslides	1.5 m	100.000	Chacón-Barrantes et al., 2013 Lehfeldt et al., 2007
Erupting or collapsing volcanoes	insignificant	beyond practical (design) relevance	Abadie et al., 2020
Meteorite impacts	unknown	very unlikely	Paine, 1999
Fast moving storm fronts	1 m	10 - 50	See Section 2.5.1 Sibley et al., 2021

C.3 Tsunami propagation in Dutch estuaries

No information was found in literature on the propagation of tsunami waves from the southern part of the North Sea into shallow bays or estuaries, such as the Western Scheldt or the Ems estuary. However, it is expected that the tsunami wave height will become lower due to dissipation while propagating into these shallow estuaries (see also Section 2.4.2).

C.4 Conclusions

The literature study on tsunamis potentially affecting the Dutch coast showed that either a landslide in the northern part of the North Sea or a local earthquake-generated tsunami in the southern part of the North Sea can result in maximum wave heights of between 1.5 – 2 m. The probability of occurrence of such events are however very low (about once in 100.000 years). Other tsunamigenic sources, such as from earthquakes at remote subduction zones, volcanoes or meteorites, are not expected to result in significant tsunami wave heights at the Dutch coast. The most probable cause of ‘tsunami’ wave heights of up to 1m at the Dutch coast are from fast moving storm fronts (meteo-induced long waves or meteotsunamis). In shallow estuaries such as the Western Scheldt or the Ems estuary, it is expected that the tsunami wave height will become lower due to dissipation, however, no information is yet available to confirm this.

C.5 References

Abadie et al., 2020. La Palma landslide tsunami: calibrated wave source and assessment of impact on French territories. Nat. Hazards Earth Syst. Sci., 20.

Baptista, M.A., Miranda, J.M., Chierici, F. and Zitellini, N., 2003. New study of the 1755 earthquake source based on multi-channel seismic survey data and tsunami modelling. Natural Hazards and Earth System Sciences, 3: 333-340.

Bijl, 1993. Tsunami golven in het Noordzee gebied. Master Thesis. Technische Universiteit Delft.

Bondevik et al., 2005. The Storegga Slide tsunami-comparing field observations with numerical simulations, Marine and Petroleum. Geology 22.

Bork et al., 2007. Tsunami - a study regarding the North Sea coast. Berichte des Bundesamtes für Seeschifffahrt und Hydrographie Nr. 41/2007.

Chacón-Barrantes et al., 2013. Several tsunami scenarios at the North Sea and their consequences at the German Bught. Science of tsunami hazards. ISSN 8755-6839. Journal of Tsunami Society International. Vol. 32, No. 1.

DEFRA, 2005. The threat posed by tsunami to the UK. British Geological Survey, UK Met Office, Proudman Oceanographic Laboratory, HR Wallingford.

De Jong, 2004. Origin and prediction of seiches in Rotterdam harbour basins. PhD Thesis, Delft University, Faculty of Civil Engineering and Geosciences. SBN 90-9017925-9.

Gaffney et al. 2020: https://www.mdpi.com/2076-3263/10/7/270.

Lehfeldt et al., 2007. Propagation of a Tsunami-Wave in the North Sea. Die Küste, 72 (2007), 105-123.

Løvholt et al., 2020. On the landslide tsunami uncertainty and hazard. Landslides (2020) 17:2301–2315.DOI 10.1007/s10346-020-01429-z.

Van Malde, 1990. Onderzoek naar mogelijke beïnvloeding van Nederlandse getij-waterstanden door aardbevingen en naar historische “Moerzeeën”, Nota Rijkswaterstaat GWAO-90.009.

NOAA, 2023. https://www.noaa.gov/jetstream/tsunamis/tsunami-generation-landslides

Paine, 1999. Asteroid impacts: the extra hazard due to tsunami. Science of Tsunami Hazards, Vol 17, No. 3 (1999).

Sibley et al., 2021. Convective rear-flank downdraft as driver for meteotsunami along English Channel and North Sea coasts 28–29 May 2017. Natural Hazards 106(1-2):1-21. DOI: 10.1007/s11069-020-04328-7.

Sousa et al., 1992. Laboratorio Nacional de Engenharia Civil. Report 36/92-NDA, Lisbon.

Twigt and Blaas, 2007. Storegga tsunami simulations. R&D Coastal Flooding. Report Z3929. Delft Hydraulics.

Ward and Day, 2001. Cumbre Vieja Volcano -- Potential collapse and tsunami at La Palma, Canary Islands. American Geophysical Union. Paper number 2001GL000000.

Deltares is an independent institute for applied research in the field of water and subsurface. Throughout the world, we work on smart solutions for people, environment and society.

Deltares

www.deltares.nl